Biogeosciences Discuss., doi:10.5194/bg-2017-125, 2017
Manuscript under review for journal Biogeosciences
Discussion started: 12 April 2017

High organic inputs explain shallow and deep SOC storage in a long-term agroforestry system – Combining experimental and modeling approaches.

Rémi Cardinael[a,b,c*], Bertrand Guenet[d], Tiphaine Chevallier[a], Christian Dupraz[e], Thomas Cozzi[b], Claire Chenu[b]

[a] IRD, UMR Eco&Sols, Montpellier SupAgro, 2 place Viala, 34060 Montpellier, France
[b] AgroParisTech, UMR Ecosys, Avenue Lucien Brétignières, 78850 Thiverval-Grignon, France
[c] CIRAD, UPR AIDA, Avenue d'Agropolis, 34398 Montpellier, France (present address)
[d] Laboratoire des Sciences du Climat et de l'Environnement, UMR CEA-CNRS-UVSQ, CE L'Orme des Merisiers, 91191 Gif-Sur-Yvette, France
[e] INRA, UMR System, Montpellier SupAgro, 2 place Viala, 34060 Montpellier, France
* Corresponding author. Tel.: +33 04.67.61.53.08. E-mail address: remi.cardinael@cirad.fr

Keywords: priming effect, deep roots, deep soil organic carbon, spatial heterogeneity, silvoarable system, crop yield, SOC modeling

Abstract

Agroforestry is an increasingly popular farming system enabling agricultural diversification and providing several ecosystem services. In agroforestry systems, soil organic carbon (SOC) stocks are generally increased, but it is difficult to disentangle the different factors responsible for this storage. Organic carbon (OC) inputs to the soil may be larger, but SOC decomposition rates may be modified owing to microclimate, physical protection, or priming effect from roots, especially at depth. We used an 18-year-old silvoarable system associating hybrid walnut trees (*Juglans regia* × *nigra*) and durum wheat (*Triticum turgidum* L. subsp. *durum*), and an adjacent

Biogeosciences Discuss., doi:10.5194/bg-2017-125, 2017
Manuscript under review for journal Biogeosciences
Discussion started: 12 April 2017

agricultural control plot to quantify all OC inputs to the soil - leaf litter, tree fine root senescence, crop residues, and tree row herbaceous vegetation -, and measure SOC stocks down 2 m depth at varying distances from the trees. We then proposed a model that simulates SOC dynamics in agroforestry accounting for both the whole soil profile and the lateral spatial heterogeneity.

OC inputs to soil were increased by about 40% (+ 1.11 t C ha^{-1} yr^{-1}) down to 2 m depth in the agroforestry plot compared to the control, resulting in an additional SOC stock of 6.3 t C ha^{-1} down to 1 m depth. The model described properly the measured SOC stocks and distribution with depth. It showed that the increased inputs of fresh biomass to soil explained the observed additional SOC storage in the agroforestry plot. Moreover, modeling revealed a strong priming effect that would reduce the potential SOC storage due to higher organic inputs in the agroforestry system by 75 to 90%. This result questions the potential of soils to store large amounts of carbon, especially at depth. Deep-rooted trees modify OC inputs to soil, a process that deserves further studies given its potential effects on SOC dynamics.

1 Introduction

Agroforestry systems are complex agroecosystems combining trees and crops or pastures within the same field (Nair, 1993, 1985; Somarriba, 1992). More precisely, silvoarable systems associate parallel tree rows with annual crops. Some studies showed that these systems could be very productive, with a land equivalent ratio (Mead and Willey, 1980) reaching up to 1.3 (Graves et al., 2007). Silvoarable systems may therefore produce up to 30% more marketable biomass on the same area of land compared to crops and trees grown separately. This performance can be explained by a better use of water, nutrients and light by the agroecosystem throughout the year. Trees grown in silvoarable systems usually grow faster than the same trees grown in forest ecosystems, because of their lower density, and because they also benefit from

the crop fertilization (Balandier and Dupraz, 1999; Chaudhry et al., 2003; Chifflot et al., 2006). In temperate regions, farmers usually grow one crop per year, and this association of trees can extend the growing period at the field scale, especially when winter crops are intercropped with trees having a late bud break (Burgess et al., 2004). However, after several years, a decrease of crop yield can be observed in mature and highly dense plantations, especially close to the trees, due to competition between crops and trees for light, water, and nutrients (Burgess et al., 2004; Dufour et al., 2013; Yin and He, 1997).

Part of the additional biomass produced in agroforestry is used for economical purposes, such as timber or fruit production. Leaves, tree fine roots, pruning residues and the herbaceous vegetation growing in the tree rows will usually return to the soil, contributing to a higher input of organic carbon (OC) to the soil compared to an agricultural field (Peichl et al., 2006).

In such systems, the observed soil organic carbon (SOC) stocks are also generally higher compared to a cropland (Albrecht and Kandji, 2003; Kim et al., 2016; Lorenz and Lal, 2014). Cardinael *et al.*, (2017) measured a mean SOC stock accumulation rate of 0.24 (0.09-0.46) t C ha^{-1} yr^{-1} at 0-30 cm depth in several silvoarable systems compared to agricultural plots in France. Higher SOC stocks were also found in Canadian agroforestry systems, but measured only to 20 cm depth (Bambrick et al., 2010; Oelbermann et al., 2004; Peichl et al., 2006).

To our knowledge, we are still not able to disentangle the factors responsible for such a higher SOC storage. This SOC storage might be due to higher OC inputs but it could also be favored by a modification of the SOC decomposition owing to a change in SOC physical protection (Haile et al., 2010), and/or in soil temperature and moisture.

The introduction of trees in an agricultural field modifies the amount, but also the distribution of fresh organic carbon (FOC) input to the soil, both vertically and horizontally (Bambrick et al., 2010; Howlett et al., 2011; Peichl et al., 2006). FOC inputs from the trees decrease with increasing distance from the trunk and with soil depth (Moreno et al., 2005). On the contrary,

crop yield usually increases with increasing distance from the trees (Dufour et al., 2013; Li et al., 2008). Therefore, the proportions of FOC coming from both the crop residues and the trees change with distance from the trees, soil depth, and time.

Tree fine roots (diameter ≤ 2 mm) are the most active part of root systems (Eissenstat and Yanai, 1997) and play a major role in carbon cycling. In silvoarable systems, tree fine root distribution within the soil profile is strongly modified due to the competition with the crop, inducing a deeper rooting compared to trees grown in forest ecosystems (Cardinael et al., 2015a; Mulia and Dupraz, 2006). Deep soil layers may therefore receive significant OC inputs from fine root mortality and exudates. Root carbon has a higher mean residence time in the soil compared to shoot carbon (Kätterer et al., 2011; Rasse et al., 2006), presumably because root residues are preferentially stabilized within microaggregates or adsorbed to clay particles. Moreover, temperature and moisture conditions are more buffered in the subsoil than in the topsoil. The microbial biomass is also smaller at depth (Eilers et al., 2012; Fierer et al., 2003), and the spatial segregation with organic matter is larger (Salomé et al., 2010) resulting in lower decomposition rates. Deep root carbon input in the soil could therefore contribute to a SOC storage with high mean residence times. However, some studies showed that adding FOC – a source of energy for microorganisms - to the subsoil enhanced decomposition of stabilized carbon, a process called « priming effect » (Fontaine et al., 2007). The priming effect is stronger when induced by labile molecules like root exudates than by root litter coming from the decomposition of dead roots (Shahzad et al., 2015). Therefore, the net effect of deep roots on SOC stocks has to be assessed, especially in silvoarable systems.

Models are crucial as they allow virtual experiments to best design and understand complex processes in these systems (Luedeling et al., 2016). Several models have been developed to simulate interactions for light, water and nutrients between trees and crops (Charbonnier et al., 2013; Duursma and Medlyn, 2012; van Noordwijk and Lusiana, 1999; Talbot, 2011) or to

predict tree growth and crop yield in agroforestry systems (Graves et al., 2010; van der Werf et al., 2007). However, none of these models are designed to simulate SOC dynamics in agroforestry systems and they are therefore not useful to estimate SOC storage. Oelbermann & Voroney (2011) evaluated the ability of the CENTURY model (Parton et al., 1987) to predict SOC stocks in tropical and temperate agroforestry systems, but with a single-layer modeling approach (0-20 cm). The approach of modeling a single topsoil layer assumes that deep SOC does not play an active role in carbon cycling, while it was shown that deep soil layers contain important amounts of SOC (Jobbagy and Jackson, 2000), and that part of this deep SOC could cycle on decadal timescales due to root inputs or to dissolved organic carbon transport (Baisden and Parfitt, 2007; Koarashi et al., 2012). The need to take into account deep soil layers when modeling SOC dynamics is now well recognized in the scientific community (Baisden et al., 2002; Elzein and Balesdent, 1995), and several models have been proposed (Ahrens et al., 2015; Braakhekke et al., 2011; Guenet et al., 2013; Koven et al., 2013; Taghizadeh-Toosi et al., 2014). Using vertically discretized soils is particularly important when modeling the impact of agroforestry systems on SOC stocks, but to our knowledge, vertically spatialized SOC models have not yet been tested for these systems.

The aims of this study were then twofold: (i) to propose a model of soil C dynamics in agroforestry systems able to account for both vertical and lateral spatial heterogeneities and (ii) to test whether variations of fresh organic carbon (FOC) input could explain increased SOC stocks both using experimental data and model runs.

For this, we first compiled data on FOC inputs to the soil obtained in a 18-year-old agroforestry plot and in an agricultural control plot in southern France, in which SOC stocks have been recently quantified to 2 m depth (Cardinael et al., 2015b). FOC inputs comprised tree fine roots, tree leaf litter, aboveground and belowground biomass of the crop and of the herbaceous

Biogeosciences Discuss., doi:10.5194/bg-2017-125, 2017
Manuscript under review for journal Biogeosciences
Discussion started: 12 April 2017

126 vegetation in the tree rows. We compiled recently published data for FOC inputs (Cardinael et
127 al., 2015a; Germon et al., 2016), and measured the others (Table 1).
128
129 We then modified a two pools model proposed by Guenet *et al.*, (2013), to create a spatialized
130 model over depth and distance from the tree, the CARBOSAF model (soil organic CARBOn
131 dynamics in Silvoarable AgroForestry systems). Based on data acquired since the tree planting
132 in 1995 (crop yield, tree growth), and on FOC inputs, we modeled SOC dynamics to 2 m depth
133 in both the silvoarable and agricultural control plot. We evaluated the model against measured
134 SOC stocks along the profile and used this opportunity to test the importance of priming effect
135 (*PE*) for deep soil C dynamics in a silvoarable system. The performance of the two pools model
136 including *PE* was also compared with a model version including three OC pools.
137
138 **2 Materials and methods**
139 **2.1 Study site**
140 The experimental site is located at the Restinclières farm Estate in Prades-le-Lez, 15 km North
141 of Montpellier, France (longitude 04°01' E, latitude 43°43' N, elevation 54 m a.s.l.). The
142 climate is sub-humid Mediterranean with an average temperature of 15.4°C and an average
143 annual rainfall of 973 mm (years 1995–2013). The soil is a silty and carbonated (pH = 8.2) deep
144 alluvial Fluvisol (IUSS Working Group WRB, 2007). In February 1995, a 4.6 hectare
145 silvoarable agroforestry plot was established with the planting of hybrid walnut trees (*Juglans*
146 *regia* × *nigra* cv. NG23) at a density of 192 trees ha^{-1} but later thinned to 110 trees ha^{-1}. Trees
147 were planted at 13 m × 4 m spacing, and tree rows are East–West oriented. The cultivated alleys
148 are 11 m wide. The remaining part of the plot (1.4 ha) was kept as an agricultural control plot.
149 Since the tree planting, the agroforestry alleys and the control plot were managed in the same
150 way. The associated crop is most of the time durum wheat (*Triticum turgidum* L. subsp. *durum*),

except in 1998, 2001 and 2006, when rapeseed (*Brassica napus* L.) was cultivated, and in 2010 and 2013, when pea (*Pisum sativum* L.) was cultivated. The soil is ploughed to a depth of 0.2 m before sowing, and the wheat crop is fertilized with an average of 120 kg N ha^{-1} yr^{-1}. Crop residues (wheat straw) are also exported, but about 25% remain on the soil. Tree rows are covered by spontaneous herbaceous vegetation. Two successive herbaceous vegetation types occur during the year, one in summer and one in winter. The summer vegetation is mainly composed of *Avena fatua* L., and is 1.5 m tall. In winter, the vegetation is a mix of *Achillea millefolium* L., *Galium aparine* L., *Vicia* L., *Ornithogalum umbellatum* L. and *Avena fatua* L, and is 0.2 m tall.

Table 1. Synthesis of the different field and laboratory data available or measured, and their sources.

Description of the data	Source
Soil texture, bulk densities, SOC stocks	Cardinael *et al.*, (2015a)
Soil temperature and soil moisture	Measured
Tree growth (DBH)	Measured
Tree wood density	(Talbot, 2011)
Tree fine root biomass	Cardinael *et al.*, (2015b)
Tree fine root turnover	Germon *et al.*, (2016)
Crop yield and crop ABG biomass	Dufour *et al.*, (2013) and measured
Crop root biomass	Prieto *et al.*, (2015) and measured
Tree row herbaceous vegetation – ABG biomass	Measured
Tree row herbaceous vegetation – root biomass	Measured
Biomass carbon concentrations	Measured
Potential decomposition rate of roots	Prieto *et al.*, (2016a)
HSOC potential decomposition rate	Measured

DBH: Diameter at Breast Height; ABG: aboveground; OC: organic carbon; HSOC: humified soil organic carbon.

2.2 Organic carbon stocks

2.2.1 Soil organic carbon stocks

Biogeosciences Discuss., doi:10.5194/bg-2017-125, 2017
Manuscript under review for journal Biogeosciences
Discussion started: 12 April 2017

168 SOC data have been published in Cardinael *et al.*, (2015a). Briefly, soil cores were sampled
169 down to 2 m depth in May 2013, 100 in the agroforestry plot, and 93 in the agricultural control
170 plot. SOC concentrations, SOC stocks, and soil texture were measured for ten soil layers (0.0-
171 0.1, 0.1-0.3, 0.3-0.5, 0.5-0.7, 0.7-1.0, 1.0-1.2, 1.2-1.4, 1.4-1.6, 1.6-1.8, and 1.8-2.0 m). In the
172 agroforestry plot, 40 soil cores were taken in the tree rows, while 60 were sampled in the alleys
173 at varying distances from the trees. Soil organic carbon stocks were quantified on an equivalent
174 soil mass basis (Ellert and Bettany, 1995).
175
176 **2.2.2 Tree aboveground and stump carbon stocks**
177 Three hybrid walnuts were chopped down in 2012. The trunk circumference was measured
178 every meter up to the maximum height of the tree to estimate its volume. The trunk biomass
179 was estimated by multiplying the trunk volume by the wood density that was measured at 616
180 kg m^{-3} during a previous work at the same site (Talbot, 2011). Then, branches were cut, the
181 stump was uprooted, and they were weighted separately. Samples were brought to the
182 laboratory to determine the moisture content, which enabled calculation of the branches and the
183 stump dry mass.
184
185 **2.3 Measurements of organic carbon inputs in the field**
186 **2.3.1 Carbon inputs from tree fine root mortality**
187 The tree fine root (diameter ≤ 2 mm) biomass was quantified and coupled with an estimate of
188 the tree fine root turnover in order to predict the carbon input to the soil from the tree fine root
189 mortality. A detailed description of the methods used to estimate the tree fine root biomass can
190 be found in Cardinael *et al.*, (2015b). In March 2012, a 5 (length) × 1.5 (width) × 4 m (depth)
191 pit was open in the agroforestry plot, perpendicular to the tree row, at the North of the trees.
192 The tree fine root distribution was mapped down 4 m depth, and the tree fine root biomass was

quantified in the tree row and in the alley. Only results concerning the first two meters of soil, among those obtained by Cardinael *et al.*, (2015b) will be presented here.

In July 2012, sixteen minirhizotrons were installed in the agroforestry pit, at 0, 1, 2.5 and 4 m depth, and at two and five meters from the trees. The tree root growth and mortality was monitored during one year using a scanner (CI-600 Root Growth Monitoring System, CID, USA), and analyzed using the WinRHIZO Tron software (Régent, Canada). A detailed description of the methods and of results used to estimate the tree fine root turnover can be found in Germon *et al.*, (2016).

2.3.2 Tree litterfall

In 2009, the crowns of two walnut trees were packed with a net in order to collect the leaf biomass from September to January. The same was done in 2012 with three other walnut trees. The leaf litter was then dried, weighted and analyzed for C to quantify the leaf carbon input per tree.

2.3.3 Aboveground and belowground input from the crop

Since the tree planting in 1995, the crop yield was measured 14 times (in 1995, 2000, 2002, 2003, 2004, 2005, 2007, 2008, 2009, 2010, 2011, 2012, 2013, and 2014), while the wheat straw biomass and the total aboveground biomass were measured six times (in 2007, 2008, 2009, 2011, 2012, and 2014) in both the control and the agroforestry plot (Dufour et al., 2013), using sampling subplots of 1 m^2 each. In the control plot, five subplots have been sampled while in the agroforestry plot five transects have been sampled. Each transect was made of three subplots, 2 m North from the tree, 2 m South from the tree, and 6.5 m from the tree (middle of the alley). In March 2012, a 2 m deep pit was opened in the agricultural control plot (Prieto et al., 2015), and the root biomass was quantified to the maximum rooting depth (1.5 m). The

Biogeosciences Discuss., doi:10.5194/bg-2017-125, 2017
Manuscript under review for journal Biogeosciences
Discussion started: 12 April 2017

root:shoot ratio of durum wheat was measured in the control plot. We assumed that the crop root biomass turns out once a year, after the crop harvest.

2.3.4 Above and belowground input from the tree row herbaceous vegetation

As two types of herbaceous vegetation grow in the tree rows during the year, samples were taken in summer and winter. In late June 2014, twelve subplots of 1 m^2 each were positioned in the tree rows, around 4 walnut trees. In January 2015, six subplots of 1 m^2 each were positioned in the tree rows, around 2 walnut trees. The middle of each subplot was located at 1 m, 2 m and 3 m, respectively, from the selected walnut tree. All the aboveground vegetation was collected in each square. In the middle of each subplot, root biomass was sampled with a cylindrical soil corer (inner diameter of 8 cm). Soil was taken at three soil layers, 0.0-0.1, 0.1-0.3 and 0.3-0.5 m. In the laboratory, soil was gently washed with water through a 2 mm mesh sieve, and roots were collected. Roots from the herbaceous vegetation were easily separated manually from walnut roots, as they were soft and yellow compared to walnuts roots that were black. After being sorted out from the soil and cleaned, the root biomass was dried at 40°C and measured.

2.4 Carbon concentration measurements

All organic carbon measurements were performed with a CHN elemental analyzer (Carlo Erba NA 2000, Milan, Italy), after samples were oven-dried at 40°C for 48 hours (Table 2). Dry biomasses (t DM ha^{-1}) of each organic matter inputs were multiplied by their respective organic carbon concentrations (mg C g^{-1}) to calculate organic carbon stocks (t C ha^{-1}).

Table 2. Organic carbon concentrations and C:N ratio of the different types of biomass.

Type of biomass	Organic C concentration (mg C g^{-1})	C:N	Number of replicates

Biogeosciences Discuss., doi:10.5194/bg-2017-125, 2017
Manuscript under review for journal Biogeosciences
Discussion started: 12 April 2017

Walnut trunk	445.7 ± 1.0	159.1 ± 25.2	3
Walnut branches	428.6 ± 1.7	62.2 ± 11.7	3
Wheat straw	433.2 ± 0.7	55.5 ± 2.1	5
Wheat root	351.4 ± 19	24.8 ± 2.1	8
Walnut leaf	449.4 ± 3.7	49.1 ± 0.4	3
Walnut fine root	437.0 ± 3.3	28.6 ± 3.4	8
Summer vegetation (ABG)	448.4 ± 1.9	37.8 ± 2.2	5
Summer vegetation (roots)	314.5 ± 8.3	33.8 ± 1.7	6
Winter vegetation (ABG)	447.7 ± 5.3	11.2 ± 0.4	3
Winter vegetation (roots)	397.4 ± 5.0	24.7 ± 0.7	3

The organic matter called "vegetation" stands for the herbaceous vegetation that grows in the tree row. ABG: aboveground. Errors represent standard errors.

2.5 General description of the CARBOSAF model

2.5.1 Organic carbon decomposition

We adapted a model developed by Guenet et al. (2013) where total SOC is split in two pools, the FOC and the humified soil organic carbon (HSOC) for each soil layer (Fig. 1a). Input to the FOC pool comes from the plant litter and the distribution of this input within the profile is assumed to depend upon depth from the surface (z), distance from the tree (d), and time (t). Equations describing inputs to the FOC pool ($I_{t,z,d}$) at a given time, depth, and distance are fully explained in the Results.

The FOC mineralisation is assumed to be governed by first order kinetics, being proportional to the FOC pool, as given by:

$$\frac{\partial FOC_{t,z,d}}{\partial t} = -k_{FOC} \times FOC_{t,z,d} \times f_{clay,z} \times f_{moist,z} \times f_{temp,z} \qquad (1)$$

where $FOC_{t,z,d}$ is the FOC carbon pool (kg C m^{-2}) at a given time (t, in years), depth (z, in m) and distance (d, in m), and k_{FOC} is its decomposition rate. The potential decomposition rates of the different plant materials were assessed with a 16-week incubation experiment during a companion study at the site (Prieto et al., 2016). The decomposition rate k_{FOC} was weighted by the respective contribution of each type of plant litter as a function of the tree age, soil depth

Biogeosciences Discuss., doi:10.5194/bg-2017-125, 2017
Manuscript under review for journal Biogeosciences
Discussion started: 12 April 2017

and distance from the tree. The rate modifiers $f_{clay,z}$, $f_{moist,z}$ and $f_{temp,z}$ are functions depending respectively on the clay content, soil moisture and soil temperature at a given depth *z*, and range between 0 and 1.

The f_{clay} function originated from the CENTURY model (Parton et al., 1987):

$$f_{clay,z} = 1 - 0.75 \times Clay_z \qquad (2)$$

where $Clay_z$ is the clay fraction (ranging between 0 and 1) of the soil at a given depth *z*.

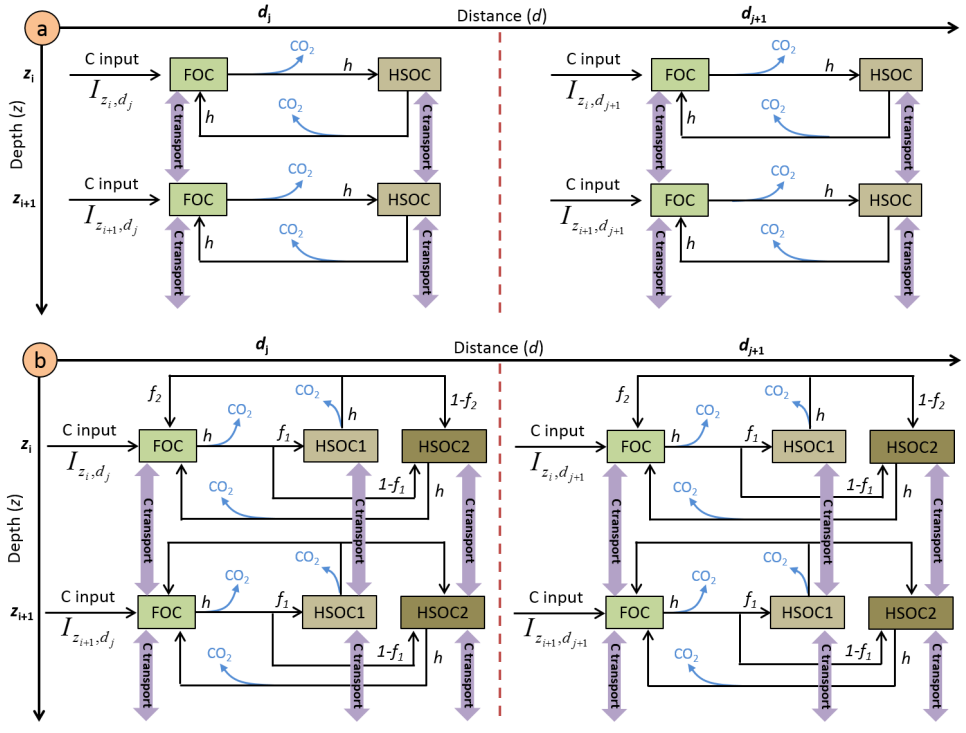

Fig. 1. Schematic representation of the pools and the fluxes of the (a) two pools model and (b) three pools model.

Biogeosciences Discuss., doi:10.5194/bg-2017-125, 2017
Manuscript under review for journal Biogeosciences
Discussion started: 12 April 2017

The $f_{moist,z}$ function originated from the meta-analysis of Moyano *et al.*, (2012) and is affected by soil properties (clay content, SOC content). Briefly, the authors fitted linear models on 310 soil incubations to describe the effect of soil moisture on decomposition. Then, they normalized such linear models between 0 and 1 to apply these functions to classical first order kinetics. All details are described in Moyano *et al.*, (2012). To save computing time, we calculated $f_{moist,z}$ only once using measured SOC stocks instead of using modelled SOC stocks and repeated the calculation at each time step.

The temperature sensitivity of the soil respiration is expressed as Q_{10}:

$$f_{temp,z} = Q_{10}^{\frac{temp_z - temp_{opt}}{10}} \quad (3)$$

with $temp_z$ being the soil temperature in K at each soil depth z and $temp_{opt}$ a parameter fixed to 304.15 K. The Q_{10} value was fixed to 2, a classical value used in models (Davidson and Janssens, 2006).

Once the FOC is decomposed, a fraction is humified (h) and another is respired as CO_2 ($1-h$) (Fig. 1a) following equations (4) and (5).

$$Humified\ FOC_{t,z,d} = h \times \frac{\partial FOC_{t,z,d}}{\partial t} \quad (4)$$

$$Respired\ FOC_{t,z,d} = (1-h) \times \frac{\partial FOC_{t,z,d}}{\partial t} \quad (5)$$

Two mathematical approaches are available in the model to describe the mineralisation of HSOC: a first order kinetics, as given by Eq. (6) or an approach developed by Wutzler & Reichstein, (2008) and by Guenet *et al.*, (2013) introducing the priming effect, i.e., the mineralisation of HSOC depends on FOC availability, and given by Eq. (7):

$$\frac{\partial HSOC_{t,z,d}}{\partial t} = -k_{HSOC,z} \times HSOC_{t,z,d} \times f_{moist,z} \times f_{temp,z} \quad (6)$$

Biogeosciences Discuss., doi:10.5194/bg-2017-125, 2017
Manuscript under review for journal Biogeosciences
Discussion started: 12 April 2017

298 $$\frac{\partial HSOC_{t,z,d}}{\partial t} = -k_{HSOC,z} \times HSOC_{t,z,d} \times (1 - e^{-PE \times FOC_{t,z,d}}) \times f_{moist,z} \times f_{temp,z} \quad (7)$$

299 where $HSOC_{t,z,d}$ is the humified SOC carbon pool at a given time (t, in years), depth (z, in m)
300 and distance (d, in m), $k_{HSOC,z}$ is its decomposition rate (yr^{-1}) at a given depth z, and PE is the
301 priming effect parameter. The parameters $f_{moist,z}$ and $f_{temp,z}$ are functions depending respectively
302 on soil moisture and soil temperature at a given depth z, and affecting the decomposition rate
303 of HSOC. They correspond to the moisture equation from Moyano *et al.*, (2012) and to Eq. (3),
304 respectively. The decomposition rate $k_{HSOC,z}$ was an exponential law depending on soil depth
305 (z) as shown by an incubation study (see paragraph *HSOC decomposition rate* further in the
306 M&M):

307 $$k_{HSOC,z} = a \times e^{-b \times z} \quad (8)$$

308 The b parameter of this equation represented the ratio of labile C/stable C within the HSOC
309 pool. The effect of clay on HSOC decomposition was implicitly taken into account in this
310 equation as clay content increased with soil depth.
311 A fraction of decomposed HSOC returns to the FOC assuming that part of the HSOC
312 decomposition products is as labile as FOC (h) and another is respired as CO_2 (Fig. 1a) in the
313 two pools model.
314
315 Finally, we also developed an alternative version of the model with three pools by splitting the
316 HSOC pools into two pools with different turnover rates, HSOC2 being more stabilized than
317 HSOC1 (Fig. 1b). The non-respired decomposed FOC is split between HSOC1 and HSOC2
318 following a parameter f_1. The non-respired decomposed HSOC1 is split between HSOC2 and
319 FOC following a parameter f_2 whereas non-respired decomposed HSOC2 is only redistributed
320 into the FOC pools. The decomposition of HSOC1 and HSOC2 both follow the equation (8)
321 but with different parameter values for a.
322

Biogeosciences Discuss., doi:10.5194/bg-2017-125, 2017
Manuscript under review for journal Biogeosciences
Discussion started: 12 April 2017

2.5.2 Carbon transport mechanisms

The transport of C between the different soil layers was represented by both advection and diffusion mechanisms (Elzein and Balesdent, 1995), which have been shown to usually describe well the C transport in soils (Bruun et al., 2007; Guenet et al., 2013). The advection represents the C transport due to the water infiltration in the soil, while the diffusion represents the C transport due to the fauna activity. The same transport coefficients were applied to the two C pools, FOC and HSOC.

The advection is defined by:

$$F_A = A \times C \qquad (9)$$

where F_A is the flux of C transported downwards by advection, and A is the advection rate (mm yr^{-1}).

The diffusion is represented by the Fick's law:

$$F_D = -D \times \frac{\partial^2 C}{\partial z^2} \qquad (10)$$

where F_D is the flux of C transported downwards by diffusion, $-D$ the diffusion coefficient (cm^2 yr^{-1}) and C the amount of carbon in the pool subject to transport (FOC or HSOC).

To represent the effect of soil tillage ($z \leq 0.2$ m), we added another diffusion term using the Fick's law but with a value of D several orders of magnitude higher to represent the mixing due to tillage. It must be noted that no tillage effect on the decomposition was represented here because of the large unknowns on these aspects (Dimassi et al., 2013; Virto et al., 2012).

In this model, the flux of C transported downwards by the advection and diffusion (F_{AD}) was represented as the sum of both mechanisms, following Elzein & Balesdent (1995):

Biogeosciences Discuss., doi:10.5194/bg-2017-125, 2017
Manuscript under review for journal Biogeosciences
Discussion started: 12 April 2017

348 $$F_{AD} = F_A + F_D \qquad (11)$$

349

350 The FOC and HSOC pools dynamics in the two pools model correspond to:

351 $$\frac{\partial FOC}{\partial t} = I_{t,z,d} + \frac{\partial F_{AD}}{\partial z} + h \times \frac{\partial HSOC_{t,z,d}}{\partial t} - \frac{\partial FOC_{t,z,d}}{\partial t} \qquad (12)$$

352 $$\frac{\partial HSOC}{\partial t} = \frac{\partial F_{AD}}{\partial z} + h \times \frac{\partial FOC_{t,z,d}}{\partial t} - \frac{\partial HSOC_{t,z,d}}{\partial t} \qquad (13)$$

353

354 Finally, the FOC, HSOC1 and HSOC2 pools dynamics in the three pools model correspond to:

355 $$\frac{\partial FOC}{\partial t} = I_{t,z,d} + \frac{\partial F_{AD}}{\partial z} + h \times f_2 \times \frac{\partial HSOC1_{t,z,d}}{\partial t} + h \times \frac{\partial HSOC2_{t,z,d}}{\partial t} - \frac{\partial FOC_{t,z,d}}{\partial t} \qquad (14)$$

356 $$\frac{\partial HSOC1}{\partial t \partial} = \frac{\partial F_{AD}}{\partial z} + h \times f_1 \times \frac{\partial FOC_{t,z,d}}{\partial t} - \frac{\partial HSOC1_{t,z,d}}{\partial t} \qquad (15)$$

357 $$\frac{\partial HSOC2}{\partial t} = \frac{\partial F_{AD}}{\partial z} + h \times (1 - f_1) \times \frac{\partial FOC_{t,z,d}}{\partial t} + h \times (1 - f_2) \times \frac{\partial HSOC1_{t,z,d}}{\partial t}$$

358 $$- \frac{\partial HSOC2_{t,z,d}}{\partial t} \qquad (16)$$

359

360 **2.5.3 Depth dependence of HSOC potential decomposition rates**

361 The shape of the function (i.e. the *b* parameter) describing the HSOC potential decomposition
362 rate (Eq. (8)) was determined by incubating soils from the control, the alley and the tree row,
363 and from different soil layers (0.0-0.1, 0.1-0.3, 0.7-1.0 and 1.6-1.8 m). Soils were sieved at 5
364 mm, and incubated during 44 days at 20°C at a water potential of -0.03 MPa. Evolved CO_2 was
365 measured using a micro-GC at 1, 3, 7, 14, 21, 28, 35, 44 days. The three first measurement
366 dates corresponded to a pre-incubation period and were not included in the analysis. For a given
367 depth, the cumulative mineralised SOC was expressed as a percentage of total SOC and was
368 plotted against the incubation time. The slopes represented the potential SOC mineralisation
369 rate at a given soil depth and location. The potential SOC mineralisation rates were then plotted

against soil depth (Fig. S1). We used the soil incubations to determine only the *b* parameter of the curve: with such short term incubations, the SOC decomposition rate over the soil profile is overestimated because the CO_2 measured during the incubations mainly originates from the labile C pool. The *a* parameter was optimized following the procedure described further.

2.6 Boundary conditions of the CARBOSAF model

2.6.1 Annual aggregates of soil temperature and soil moisture

In April 2013, eight soil temperature and moisture sensors (Campbell CS 616 and Campbell 107, respectively) were installed in the agroforestry plot at 0.3, 1.3, 2.8 and 4.0 m depth, and at 2 and 5 m from the trees. Soil temperature and moisture were measured for 11 months.

The mean annual soil temperature in the agroforestry plot was described by the following equation:

$$T = -0.89 \times z + 288.24 \quad (R^2 = 0.99) \quad (17)$$

where *T* is the soil temperature (K) and *z* is the soil depth (m).

The mean annual soil moisture was described with the following equation:

$$\theta = 0.05 \times z + 0.28 \quad (R^2 = 0.99) \quad (18)$$

where θ is the soil volumetric moisture (cm cm^{-3}) and *z* is the soil depth (m).

Due to a lack of data in the agricultural plot, we assumed that the soil temperature and the soil moisture were the same in the agroforestry tree rows, alleys and in the control plot, but we further performed a sensitivity analysis of the model on these two parameters.

2.6.2 Interpolation of tree growth

The tree growth has been measured in the field since the establishment of the experiment. We used the diameter at breast height (*DBH*) as a surrogate of the tree growth preferentially to the

tree height as the field measurements were more accurate. Indeed, *DBH* is easier to measure than height, especially when trees are getting older. To describe the temporal dynamic of *DBH* since the tree planting, a linear equation was fitted on the data.

2.6.3 Change of tree litterfall over time

For the five walnut trees where the leaf biomass was quantified, *DBH* was also measured. The ratio between the leaf biomass and *DBH* was then calculated for the five replicates. A linear relationship between the leaf biomass and *DBH* was then considered to describe the increase of the leaf litter C input with the tree growth.

2.6.4 Tree fine root C input from mortality

A decreasing exponential function was fitted on the root biomass data obtained from the pit in 2012 to describe total fine root biomass (*TFRB*) down to 2 m depth as a function of distance from the tree. We considered a linear increase of *TFRB* with increasing *DBH*, and a linear regression was performed between *TFRB* in 2012 and *TFRB* in 1996, the first year after planting (biomass considered as negligible). A changing distribution of tree fine roots within the soil profile was taken into account with increasing distance to the tree. For this purpose, exponential functions ($a \times e^{-b \times z}$) were fitted in the alley every 0.5 m distance, and a linear regression was fitted between their coefficients a and b and distance from the tree. However, the distribution of *TFRB* within the soil profile and with the distance to the tree was considered constant with time. To finally estimate the tree fine root input due to the mortality, *TFRB* was multiplied by the measured root turnover.

2.6.5 Aboveground and belowground input from the crop

As there were more crop yield measurements than straw biomass measurements, the effect of agroforestry on the crop yield with time was used as an estimate for change in the aboveground and belowground wheat biomass.

For this, the relative yield ($Rel\ Y_{AF}$) in the agroforestry system was calculated for each year as the ratio between the agroforestry yield and the control yield. A linear regression was then fitted between the relative yield and the *DBH*. The variation of crop yield with distance from the trees was described with a quadratic equation. But as we aimed to predict SOC stocks up to 6.5 m distance from the trees (middle of the alley), a linear increase of crop yield with increasing distance from the tree gave similar results as the quadratic equation over the 6.5 m distance and was more parsimonious. Finally, the ratio between the straw biomass and the crop yield was calculated as the average of the six measurements, and was considered constant with time. This ratio was used to convert crop yield into straw biomass.

To estimate fine root biomass of the crop, we hypothesized that the root:shoot ratio of the durum wheat was the same in both the agroforestry and agricultural plot, in the absence of any published data on the matter. The wheat root distribution within the soil profile as a function of total wheat root biomass was described by an exponential fit. Since the same maximum rooting depth of the crop was observed in the agroforestry plot and in the control plot, we inferred that the wheat root distribution within the soil profile was not modified by agroforestry, but only its biomass.

2.6.6 Aboveground and belowground input from herbaceous vegetation in the tree rows

We fitted an exponential function to describe the herbaceous root biomass with depth. We assumed for simplification that the aboveground and belowground biomasses of the herbaceous vegetation in the tree row were constant over time.

Biogeosciences Discuss., doi:10.5194/bg-2017-125, 2017
Manuscript under review for journal Biogeosciences
Discussion started: 12 April 2017

444 **2.7 Optimization procedure**

445 Five parameters were optimized with a Bayesian statistical method (Santaren et al., 2007;
446 Tarantola, 1987, 2005). These parameters were *A*, the advection rate, *D*, the diffusion
447 coefficient, *h* the humification yield, *a* the coefficient of the k_{HSOC} rate from Eq. (10), and *PE*
448 the priming coefficient. The model was fitted to the SOC stocks data using a Bayesian curve
449 fitting method described in Tarantola (1987), after a conversion from SOC stocks in kg C m^{-2}
450 to SOC stocks in kg m^{-3} due to the different soil layers' thickness. We aimed to find a parameter
451 set that minimizes the distance between model outputs and the corresponding observations,
452 considering model and data uncertainties, and prior information on parameters. With the
453 assumption of Gaussian errors for both the observations and the prior parameters, the optimal
454 parameter set corresponds to the minimum of the cost function $\boldsymbol{J}(\boldsymbol{x})$:

455 $$\boldsymbol{J}(\boldsymbol{x}) = 0.5 \times \left[(\boldsymbol{y} - \boldsymbol{H}(\boldsymbol{x}))^t \times \boldsymbol{R}^{-1} \times \left(\boldsymbol{y} - \boldsymbol{H}(\boldsymbol{x})\right) + (\boldsymbol{x} - \boldsymbol{x}_b)^t \times \boldsymbol{P}_b{}^{-1} \times (\boldsymbol{x} - \boldsymbol{x}_b)\right] \quad (19)$$

456 that contains both the mismatch between modelled and observed SOC stock and the mismatch
457 between a priori and optimized parameters. $\boldsymbol{x}$ is the vector of unknown parameters, $\boldsymbol{x}_b$ the
458 vector of a priori parameter values, $\boldsymbol{H}()$ the model and y the vector of observations. The
459 covariance matrices $\boldsymbol{P}_b$ and $\boldsymbol{R}$ describe a priori uncertainties on parameters, and observations,
460 respectively. Both matrices are diagonal as we suppose the observation uncertainties and the
461 parameter uncertainties to be independent. To determine an optimal set of parameters which
462 minimizes $\boldsymbol{J}(\boldsymbol{x})$, we used the BGFS gradient-based algorithm (Tarantola, 1987). We performed
463 30 optimizations starting with different parameter prior values to check that the results did not
464 correspond to a local minimum. To optimize the parameters we only used the data coming from
465 the control plot.

466

467 **2.8 Comparison of models**

Biogeosciences Discuss., doi:10.5194/bg-2017-125, 2017
Manuscript under review for journal Biogeosciences
Discussion started: 12 April 2017

468 Model predictions with and without priming effect were compared calculating the coefficients
469 of determination, root mean square errors (RMSE) and Bayesian information criteria (BIC).

470 $$RMSE = \sqrt{\frac{1}{N}\sum_{i=1}^{N}(x_i - \bar{x})^2} \qquad (20)$$

471 where i is the number of observations (1 to N), x_i is the predicted value and $\bar{x}$ is the mean
472 observed value.

473 $$BIC = N \times \ln(MSD) + k \times \ln(N) \qquad (21)$$

474 where *N* is the number of observations, *MSD* is the mean squared deviation, and *k* is the number
475 of model parameters.

476

477 The model was run at a yearly time step using mean annual soil temperature and moisture and
478 annual C inputs to the soil. SOC pools were initialized after a spin-up of 5000 years in the
479 control plot. Measured SOC stocks in 2013 in the control plot were used for the spin up. The
480 associated uncertainty was estimated with the 93 soil cores sampled in the control plot (see
481 section 2.2.1). Due to a lack of relevant data, we assumed that the climate and the land use were
482 the same for the last 5000 years, and that SOC stocks in the control plot were at equilibrium.
483 Therefore, SOC stocks at the end of the spin-up equaled SOC stocks in the control plot. Three
484 different spin-ups were performed, corresponding to the three different models that were used:
485 one spin-up with the two pools model without the priming effect, one spin-up with the two
486 pools model with the priming effect, and one spin-up with the three pools model. In the
487 agroforestry, the model was run from the ground (0 m) to 2 m depth, and from the tree (0 m) to
488 6.5 m from the tree (middle of the alley). The model was applied separately across locations of
489 a tree-distance gradient having varying OC inputs, each soil column was considered
490 independent from another. The model was then run from t_0 to t_{18} (years) after tree planting. The

Biogeosciences Discuss., doi:10.5194/bg-2017-125, 2017
Manuscript under review for journal Biogeosciences
Discussion started: 12 April 2017

491 spatial resolution was 0.1 m both vertically and horizontally. The model was developed using
492 R 3.1.1 (R Development Core Team, 2013).
493
494 **2.9 Estimation of the priming intensity and its impact on SOC storage**
495 In equation (7), the priming effect (*PE*) is considered as a control of the FOC on the HSOC
496 decomposition and not as an accelerating factor of the HSOC decomposition. This method
497 followed the Wutzler & Reichstein, (2008) approach based on the microbial biomass and
498 adapted to the FOC by Guenet *et al.*, (2013) for models without explicit microbial biomass.
499 Models able to reproduce priming effect generally need an explicit microbial biomass
500 controlling the decomposition (Blagodatsky et al., 2010; Perveen et al., 2014). The priming
501 scheme used here allows some simplifications in the model structure since an explicit
502 representation of the microbial biomass is not needed. Furthermore, at equilibrium state (i.e.
503 when the input rate is constant) the decomposition rate of a first order equation (Eq. (6)) takes
504 *PE* implicitly into account. When FOC inputs are modified, due to the tree growth for instance,
505 the *PE* intensity is modified and this effect cannot be represented by classical first order
506 kinetics. To estimate the importance of priming on SOC storage in the agroforestry plot, the
507 simulations using first order equations (Eq. (6)) can therefore not be directly compared to the
508 simulations using the FOC-dependant decomposition rate (Eq. (7)). To estimate the change of
509 SOC decomposition rate due to priming when trees are planted, the decomposition rate
510 predicted by Eq. (7) $\left(-k_{HSOC,z} \times (1 - e^{-PE \times FOC_{t,z,d}})\right)$ in the agroforestry plot has to be
511 compared to the control plot decomposition rate. Thus, to calculate the importance of priming
512 on SOC storage when trees are planted, we used the decomposition rates calculated following
513 Eq. (7) in the control plot $\left(-k_{HSOC,z} \times (1 - e^{-PE \times FOC_{t,z,d}})\right)$ and we applied this decomposition
514 rate to the agroforestry plot as a classical first order kinetics (without the FOC from the control
515 plot). This simulation corresponded to the absence of priming due to trees in the agroforestry

Biogeosciences Discuss., doi:10.5194/bg-2017-125, 2017
Manuscript under review for journal Biogeosciences
Discussion started: 12 April 2017

plot (i.e. decomposition not controlled by the FOC of the agroforestry plot). By difference with the simulation performed with the full two pools model (Eq. (7)), i.e., taking account of FOC input and priming, we calculated the priming intensity.

3 Results

3.1 Experimental results

3.1.1 Carbon stock in the walnut tree biomass

The measured aboveground (trunk + branches) and stump carbon stock of 18-year-old walnut trees are presented in Table 3.

Table 3. Carbon stocks in the aboveground biomass and in the stump of 18-year-old walnut trees (110 trees ha^{-1}).

	Tree biomass carbon stock	
	(kg C $tree^{-1}$)	(t C ha^{-1})
Trunk	55.06 ± 4.35	6.06 ± 0.48
Branches	40.98 ± 7.65	4.51 ± 0.84
Stump	21.21 ± 1.07	2.33 ± 0.12
Total	117.25 ± 8.87	12.9 ± 0.98

Errors represent standard errors.

3.1.2 Tree growth

Tree growth measurements enabled us to fit the following equation that was used in the model:

$$DBH_t \begin{cases} 0.01, & t \leq 3 \\ 0.0157 \times t - 0.0391 \ (R^2 = 0.997) & 3 < t \leq 20 \end{cases} \quad (22)$$

where DBH_t is the diameter at breast height (m) and t represents the time since tree planting (years).

3.1.3 Crop yield

Biogeosciences Discuss., doi:10.5194/bg-2017-125, 2017
Manuscript under review for journal Biogeosciences
Discussion started: 12 April 2017

The average annual crop yield in the control plot was $Y_C = 3.79 \pm 0.40$ t DM ha^{-1} for the 14 studied years. In the agroforestry plot, the average relative yield decreased linearly with time (increasing *DBH*) and was described using the following linear equation (Fig. 2):

$$Rel\ Y_{AF_t} = -93.33 \times DBH_t + 100 \qquad (R^2 = 0.12, \quad p - value = 0.02) \qquad (23)$$

where $Rel\ Y_{AF_t}$ is the average relative crop yield (%) in the agroforestry plot compared to the control plot at year *t*, and DBH_t is the diameter at breast height (m) at year *t*.

In the agroforestry plot, a linear relationship was used to describe the relative crop yield increase from the tree to the middle of the alley (Fig. 2):

$$Rel\ Y_{AF_d} = 4.39 \times d + 64.57 \quad (R^2 = 0.24), \qquad 1 < d \leq 6.5 \qquad (24)$$

where $Rel\ Y_{AF_d}$ is the relative crop yield (%) in the agroforestry plot at a distance d (m) from the tree compared to the control plot.

Finally, the crop yield in the agroforestry plot was modeled as follows:

$$Y_{AF_{t,d}} = Rel\ Y_{AF_t} \times Y_C \times Rel\ Y_{AF_d} \quad (R^2 = 0.19), \qquad 1 < d \leq 6.5 \qquad (25)$$

where $Y_{AF_{t,d}}$ is the crop yield (t DM ha^{-1}) in the agroforestry plot at the year *t* and at a distance d (m) from the tree. Because three linear equations were used to describe the crop yield in the agroforestry plot, errors were accumulated and we finally came up with a standard underestimation of the crop yield in the agroforestry plot that we corrected by multiplying our equation by 1.2.

Biogeosciences Discuss., doi:10.5194/bg-2017-125, 2017
Manuscript under review for journal Biogeosciences
Discussion started: 12 April 2017

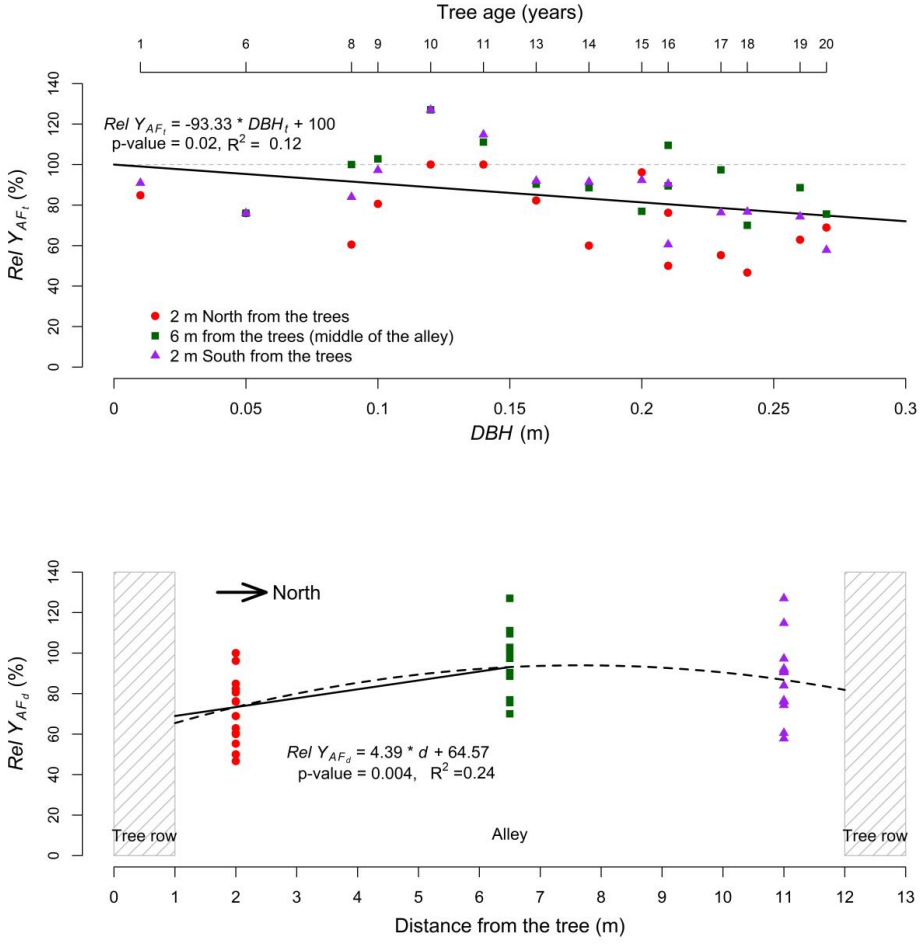

Fig. 2. Top: Relative yield ($Rel\ Y_{AF_t}$) in the agroforestry plot compared to the control plot as a function of tree growth, represented by the diameter at breast height (*DBH*) at year *t*. Bottom: Relative yield ($Y_{AF_{t,d}}$) as a function of the distance from the tree.

3.2 Carbon inputs to the FOC pool

3.2.1 Leaf litterfall Total leaf biomass was 8.96 ± 1.45 kg DM tree^{-1} and the carbon concentration of walnut leaves was 449.4 ± 3.7 mg C g^{-1} (Table 2). With a density of 110 trees ha^{-1}, leaf litterfall was estimated at 0.73 ± 0.06 t C ha^{-1} in 2012 and at the plot scale. The ratio

Biogeosciences Discuss., doi:10.5194/bg-2017-125, 2017
Manuscript under review for journal Biogeosciences
Discussion started: 12 April 2017

between leaf biomass and *DBH* was 0.0277 ± 0.0024 t C tree^{-1} m^{-1} or 3.05 t C ha^{-1} m^{-1}. The following linear relationship was therefore used in the model to describe leaf litter C input:

$$L_t = 3.05 \times DBH_t \qquad (26)$$

where L_t is the leaf litter input (t C ha^{-1}) at the year *t*, and DBH_t the diameter at breast height (m) the year *t*.

3.2.2 Tree fine root C input from mortality

In 2012, the measured tree fine root biomass was higher in the tree row than in the alley (Table 4). From 0 to 1 m distance from the tree (in the tree row), the tree fine root biomass was homogeneous and was 1.01 t C ha^{-1} down 2 m depth.

Table 4. Walnut tree fine root biomass (t C ha^{-1}) as a function of depth and distance from the trees (m).

	Tree fine root biomass (t C ha^{-1})			
	Tree row		Alley	
Soil depth (m)	[0, 1] m	]1, 2.5] m	]2.5, 4.0] m	]4.0, 5.5] m
0.0-0.1	0.08 ± 0.01	0.08 ± 0.01	0.01 ± 0.00	0.00 ± 0.00
0.1-0.3	0.14 ± 0.02	0.24 ± 0.02	0.15 ± 0.02	0.05 ± 0.01
0.3-0.5	0.22 ± 0.02	0.16 ± 0.02	0.08 ± 0.01	0.05 ± 0.01
0.5-1.0	0.35 ± 0.04	0.14 ± 0.01	0.14 ± 0.01	0.08 ± 0.01
1.0-1.5	0.15 ± 0.02	0.10 ± 0.01	0.08 ± 0.01	0.08 ± 0.01
1.5-2.0	0.07 ± 0.01	0.13 ± 0.01	0.09 ± 0.01	0.07 ± 0.01
Total	1.01 ± 0.06	0.84 ± 0.04	0.55 ± 0.03	0.34 ± 0.02

Data modified from Cardinael *et al.*, (2015b). Errors represent standard errors.

In 2012 and in the alley, the tree fine root biomass decreased with increasing distance from the tree and was represented by an exponential function:

$$TFRB = \begin{cases} 1.01, & 0 \le d \le 1 \\ 1.29 \times e^{-0.28 \times d} \quad (R^2 = 0.90), & 1 < d \le 6.5 \end{cases} \qquad (27)$$

588 where *TFRB* represents tree fine root biomass down 2 m depth (t C ha^{-1}), and *d* the distance
589 from the tree (m).
590
591 The following linear relationship was used to simulate *TFRB* as a function of tree growth:

592 $$TFRB_{t,d} = \begin{cases} 3.69 \times DBH_t, & 0 \le d \le 1 \\ 4.70 \times DBH_t \times e^{-0.28 \times d}, & 1 < d \le 6.5 \end{cases} \quad (28)$$

593 where $TFRB_t$ represents the tree fine root biomass to 2 m depth (t C ha^{-1}) at the year *t*, DBH_t the
594 diameter at breast height (m) at the year *t*, and *d* the distance to the tree (m).
595
596 A decreasing exponential function best represented the changing distribution of tree fine roots
597 within the soil profile with increasing distance to the tree:

598 $$p_{TFRB,z,d} = \begin{cases} 13.92 \times e^{-1.39 \times z} \quad (R^2 = 0.68), & 0 \le d \le 1 \\ a \times e^{-b \times z}, & 1 < d \le 6.5 \end{cases} \quad (29)$$

599 and

600 $$a = 10.31 - 1.15 \times d \quad (R^2 = 0.69) \quad (30)$$

601 $$b = -1.10 + 0.19 \times d \quad (R^2 = 0.51) \quad (31)$$

602 Finally,

603 $$p_{TFRB,z,d} = \begin{cases} 13.92 \times e^{-1.39 \times z}, & 0 \le d \le 1 \\ (10.31 - 1.15 \times d) \times e^{-(-1.10+0.19 \times d) \times z}, & 1 < d \le 6.5 \end{cases} \quad (32)$$

604 where $p_{TFRB,z,d}$ is the proportion (%) of the total tree fine root biomass (*TFRB*) at a given depth
605 *z* (m), and at a distance *d* from the tree (m).
606
607 The tree fine root turnover ranged from 1.7 to 2.8 yr^{-1} depending on fine root diameter, with an
608 average turnover of 2.2 yr^{-1} for fine roots ≤ 2 mm and to a depth of 2 m (Germon et al., 2016).
609
610 **3.2.3 Aboveground carbon input from the crop**
611 In the agroforestry plot, the carbon input to the soil from the aboveground crop biomass was:

Biogeosciences Discuss., doi:10.5194/bg-2017-125, 2017
Manuscript under review for journal Biogeosciences
Discussion started: 12 April 2017

$$ABC_{crop,t,d} = Y_{AF_{t,d}} \times (straw\ biomass{:}\ crop\ yield) \times C_{straw} \times (1 - export) \quad (33)$$

where $ABC_{crop,t,d}$ is the aboveground carbon input from the crop (t C ha^{-1}) at the year t and distance d from the tree, $Y_{AF_{t,d}}$ is the agroforestry crop yield. The average ratio between the straw biomass (t DM ha^{-1}) and the crop yield (t DM ha^{-1}) equaled 1.03 ± 0.11 (n=6). The wheat straw was exported out of the field after the harvest, but it was estimated that 25% of the straw biomass was left on the soil, thus *export*=0.75. In the control plot, $Y_{AF_{t,d}}$ was replaced by Y_C.

3.2.4 Belowground carbon input from the crop

In the agroforestry plot, the belowground crop biomass was represented by:

$$BEC_{crop,t,d} = Y_{AF_{t,d}} \times (shoot{:}\ crop\ yield) \times (root{:}\ shoot) \times C_{root} \quad (34)$$

where $BEC_{crop,t,d}$ is the belowground crop biomass (t C ha^{-1}) at the year t and at a distance d from the tree, $Y_{AF_{t,d}}$ is the agroforestry crop yield. The average ratio between the total crop aboveground biomass (*shoot*) and the crop yield equaled 2.45 ± 0.15 (n=6). In 2012, total fine root biomass was 2.29 ± 0.32 t C ha^{-1} in the control (Table 5).

Table 5. Wheat fine root biomass in the agricultural control plot in 2012.

Soil depth (m)	Wheat fine root biomass (kg C m^{-3})	(t C ha^{-1})
0.0-0.1	0.48 ± 0.05	0.48 ± 0.05
0.1-0.3	0.34 ± 0.04	0.69 ± 0.09
0.3-0.5	0.22 ± 0.04	0.44 ± 0.08
0.5-1.0	0.10 ± 0.04	0.52 ± 0.20
1.0-1.5	0.03 ± 0.04	0.17 ± 0.19
Total	-	2.29 ± 0.32

Errors represent standard errors.

Therefore, the wheat *root:shoot* ratio equaled 0.79 ± 0.12 (n=1). The carbon concentration of wheat root was C_{root} = 35.14 ± 1.90 mg C g^{-1}. In the control plot, $Y_{AF_{t,d}}$ was replaced by Y_C.

Biogeosciences Discuss., doi:10.5194/bg-2017-125, 2017
Manuscript under review for journal Biogeosciences
Discussion started: 12 April 2017

632 In 2012, no wheat roots were observed below 1.5 m, and root biomass decreased exponentially
633 with increasing depth (Table 5). The distribution of crop roots within the soil profile was
634 described as follows:

635 $$p_{CRBc,z} = \begin{cases} 26.44 \times e^{-2.59 \times z} \quad (R^2 = 0.99), & z \leq 1.5 \\ 0, & z > 1.5 \end{cases} \qquad (35)$$

636 where $p_{CRBc,z}$ is the proportion (%) of total crop root biomass in the control plot at a given
637 depth z (m).
638 The crop root turnover was assumed to be 1 yr^{-1}, root mortality occurring mainly after crop
639 harvest.
640

641 **3.2.5 Aboveground and belowground carbon inputs from the tree row herbaceous**
642 **vegetation**

643 The distance from the trees had no effect on the above and belowground biomass of the
644 herbaceous vegetation (data not shown), therefore average values are presented. The summer
645 aboveground biomass was almost three times higher than in winter, whereas the belowground
646 biomass was two times higher (Table 6). The total aboveground carbon input was 2.13 ± 0.14 t
647 C ha^{-1} yr^{-1} and the total belowground carbon input was 0.74 ± 0.05 t C ha^{-1} yr^{-1} to 0.5 m depth.
648

649 **Table 6.** Aboveground and belowground biomass of the herbaceous vegetation in the tree rows.

		Herbaceous biomass (t C ha^{-1})	
	Soil depth (m)	Summer	Winter
Aboveground	-	1.57 ± 0.11	0.56 ± 0.09
Belowground	0.0-0.1	0.22 ± 0.03	0.17 ± 0.01
	0.1-0.3	0.16 ± 0.02	0.06 ± 0.01
	0.3-0.5	0.09 ± 0.04	0.04 ± 0.01
	Total	0.46 ± 0.04	0.27 ± 0.02

650 Errors represent standard errors.
651

Biogeosciences Discuss., doi:10.5194/bg-2017-125, 2017
Manuscript under review for journal Biogeosciences
Discussion started: 12 April 2017

652 The belowground carbon input from the tree row vegetation ($BEC_{veg,z}$, t C ha^{-1}) at a given depth
653 z (m) was described by the following equation:

654 $$BEC_{veg,z} = \begin{cases} 0.44 \times e^{-3.12 \times z}, & z \leq 1.5 \\ 0, & z > 1.5 \end{cases} \quad (36)$$

655

656 **3.2.6 Organic carbon inputs and SOC stocks: a synthesis from field measurements**

657 Tree rows in the agroforestry system received two times more organic carbon (OC) inputs
658 compared to the control plot (Fig. 3), and 65% more than alleys. Globally, the agroforestry plot
659 had 41% more OC inputs to the soil than the control plot to 2 m depth (3.80 t C ha^{-1} yr^{-1}
660 compared to 2.69 t C ha^{-1} yr^{-1}). In the control plot, 85% of OC inputs are wheat root litters. In
661 the agroforestry plot, root inputs represent 71% of OC inputs in the alleys, and 50% in the tree
662 rows.

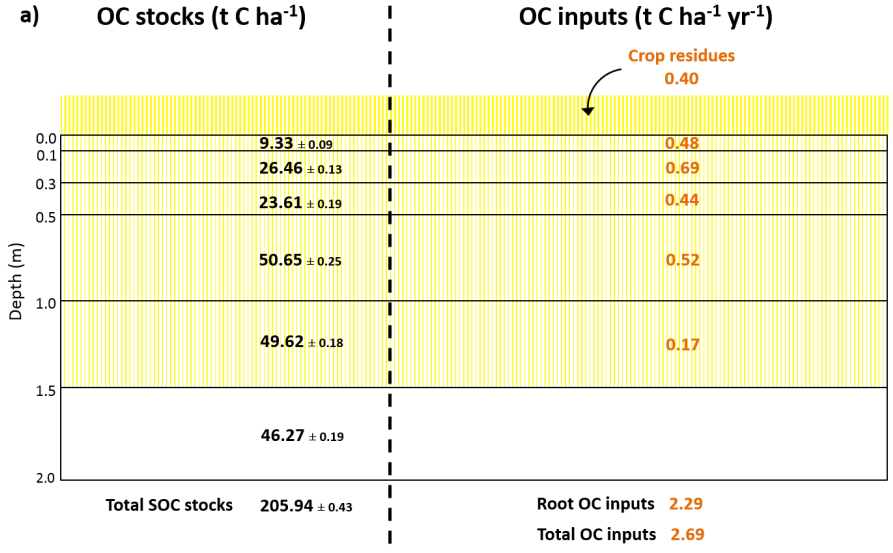

663

664

Biogeosciences Discuss., doi:10.5194/bg-2017-125, 2017
Manuscript under review for journal Biogeosciences
Discussion started: 12 April 2017

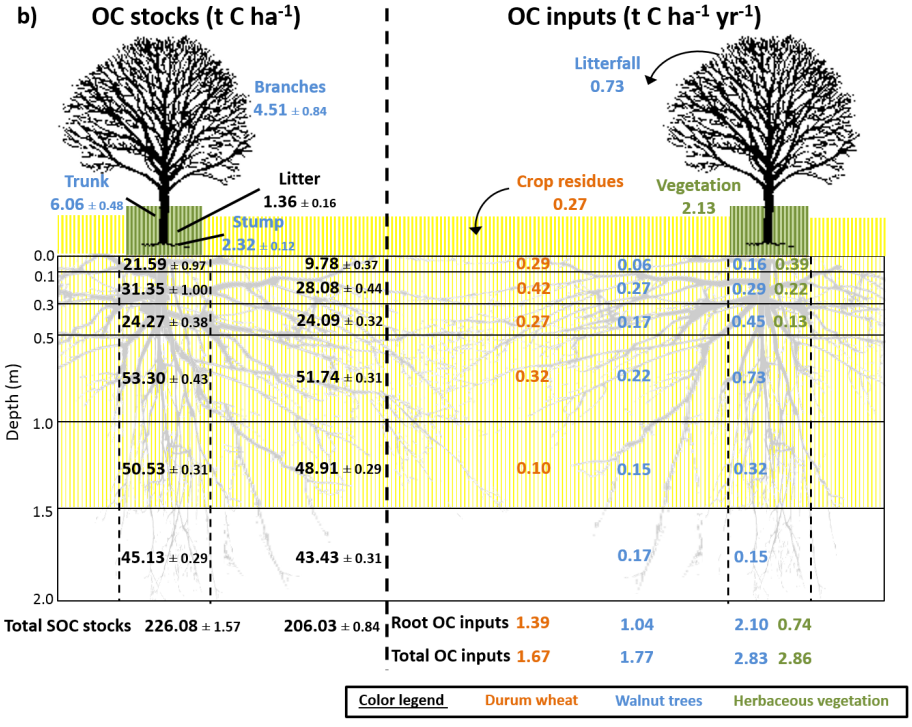

Fig. 3. Measured soil organic carbon stocks and organic carbon inputs to the soil a) in the agricultural control plot, b) in the 18-year-old agroforestry plot. Associated errors are standard errors. Values are expressed per hectare of land type (control, alley, tree row). To get the values per hectare of agroforestry, data from alley and tree row have to be weighted by their respective surface area (i.e., 84% and 16%, respectively) and then added up. OC: organic carbon; SOC: soil organic carbon. SOC stocks data are issued from Cardinael *et al.*, (2015a), data of tree root OC inputs are combined from Cardinael *et al.*, (2015b) and from Germon *et al.*, (2016).

3.3 HSOC decomposition rate

The soil incubation experiment showed that the HSOC mineralization rate decreased exponentially with depth (Fig. S1) and could be described with:

Biogeosciences Discuss., doi:10.5194/bg-2017-125, 2017
Manuscript under review for journal Biogeosciences
Discussion started: 12 April 2017

$$k_{HSOC,z} = 6.114 \times e^{-1.37 \times z} \quad (R^2 = 0.76) \qquad (34)$$

where z is the soil depth (m), and where the a (yr^{-1}) coefficient (a = 6.114) was further optimized (Table 7).

Biogeosciences Discuss., doi:10.5194/bg-2017-125, 2017
Manuscript under review for journal Biogeosciences
Discussion started: 12 April 2017

682 **Table 7.** Summary of optimized model parameters.

Model parameter	Meaning	Prior range	Posterior values ± variance (prior values)		
			2 pools - without *PE*	2 pools - with *PE*	3 pools – without *PE*
a	coefficient from Eq. (8) of the HSOC decomposition (yr^{-1})	$3.65e^{-6}$-3.65	$0.01e^{-2} \pm <10^{-4}$ ($0.01e^{-2}$)	$0.01e^{-2} \pm <10^{-4}$ ($0.01e^{-2}$)	-
a_1	coefficient from Eq. (8) of the HSOC1 decomposition (yr^{-1})	$3.65e^{-6}$-3.65	-	-	$0.01e^{-2} \pm <10^{-4}$ ($0.01e^{-2}$)
a_2	coefficient from Eq. (8) of the HSOC2 decomposition (yr^{-1})	$3.65e^{-6}$-3.65	-	-	$0.83e^{-2} \pm 0.17e^{-2}$ ($0.83e^{-2}$)
D	diffusion coefficient ($cm^2\ yr^{-1}$)	$1e^{-6}$-1	$4.62e^{-4} \pm 5.95e^{-4}$ ($9.64e^{-4}$)	$5.63e^{-4} \pm 1.42e^{-4}$ ($9.01e^{-4}$)	$5.24e^{-4} \pm 7.62e^{-4}$ ($9.64e^{-4}$)
A	advection rate ($mm\ yr^{-1}$)	$1e^{-6}$-1	$21.25e^{-4} \pm 5.02e^{-4}$ ($8.54e^{-4}$)	$6.63e^{-4} \pm 2.38e^{-4}$ ($4.27e^{-4}$)	$21.60e^{-4} \pm 2.24e^{-4}$ ($8.54e^{-4}$)
h	humification yield	0.01-1	$0.32 \pm <10^{-4}$ (0.34)	$0.25 \pm 1.00e^{-4}$ (0.13)	0.34 ± 0.03 (0.34)
PE	priming coefficient	0.1-160	-	9.66 ± 1.49 (102.95)	-
f_1	fraction of decomposed FOC entering the HSOC1 pool	0-1	-	-	0.99 ± 0.18 (0.86)
f_2	fraction of decomposed HSOC1 entering the FOC pool	0-1	-	-	$0.94 \pm 1.10e^{-3}$ (0.80)

683

684

Biogeosciences Discuss., doi:10.5194/bg-2017-125, 2017
Manuscript under review for journal Biogeosciences
Discussion started: 12 April 2017

685 **3.4 Modeling results**

686 **3.4.1 Optimized parameters and correlation matrix**

687 The optimized parameters and their prior modes are presented in Table 7. For the two pools
688 model without priming effect, the most important correlation was observed between *h* and *A*
689 which control the humification and the transport by advection. Concerning the two pools model
690 with priming effect, the most important correlations were observed between *h* and *PE* which
691 controls the effect of the FOC on HSOC decomposition, and between *h* and *A*. *A* and *PE* were
692 also positively correlated (Fig. S2). For the three pools model, f_1 and f_2 were by definition
693 negatively correlated, but f_2 and *A* were also correlated. Considering the method used to
694 optimize the parameters, these important correlation factors hinder the presentation of the
695 model output within an envelope. Therefore, we presented the model results using the optimized
696 parameter without any envelope.

697

698 **3.4.2 Modeled SOC stocks**

699 Observed SOC stocks were not well represented by the two pools model without priming effect,
700 with RMSE ranging from 1.00 to 1.07 kg C m^{-3} (Fig. 4, Table S1). The model performed better
701 when the priming effect was taken into account, with RMSE ranging from 0.41 to 0.95 kg C m^{-}
702 ^{3}, and the SOC profile was well described. The representation of SOC stocks was not improved
703 by the inclusion of a third C pool in the model. Globally, the two pools model with priming
704 effect was the best one, as shown by the BICs (Fig. 4, Table S1). For all models, SOC stocks
705 below 1 m depth were better described than above SOC stocks (Table S1). The spatial
706 distribution of SOC storage was also well described (Fig. 5), with a very high SOC stock in the
707 topsoil layer in the tree row. Most modeled SOC storage in the agroforestry plot was located in
708 the first 0.2 m depth, and SOC storage was slightly higher in the middle of the alleys than in
709 the alleys close to the tree rows.

Biogeosciences Discuss., doi:10.5194/bg-2017-125, 2017
Manuscript under review for journal Biogeosciences
Discussion started: 12 April 2017

Biogeosciences Discuss., doi:10.5194/bg-2017-125, 2017
Manuscript under review for journal Biogeosciences
Discussion started: 12 April 2017

Fig. 4. Measured and modeled soil organic carbon contents (kg C m^{-3}) in an agricultural control plot and in an 18-year-old silvoarable system with a two pools model without priming effect (no *PE*), with a two pools model with priming effect (*PE*) and with a three pools model without *PE*.

Biogeosciences Discuss., doi:10.5194/bg-2017-125, 2017
Manuscript under review for journal Biogeosciences
Discussion started: 12 April 2017

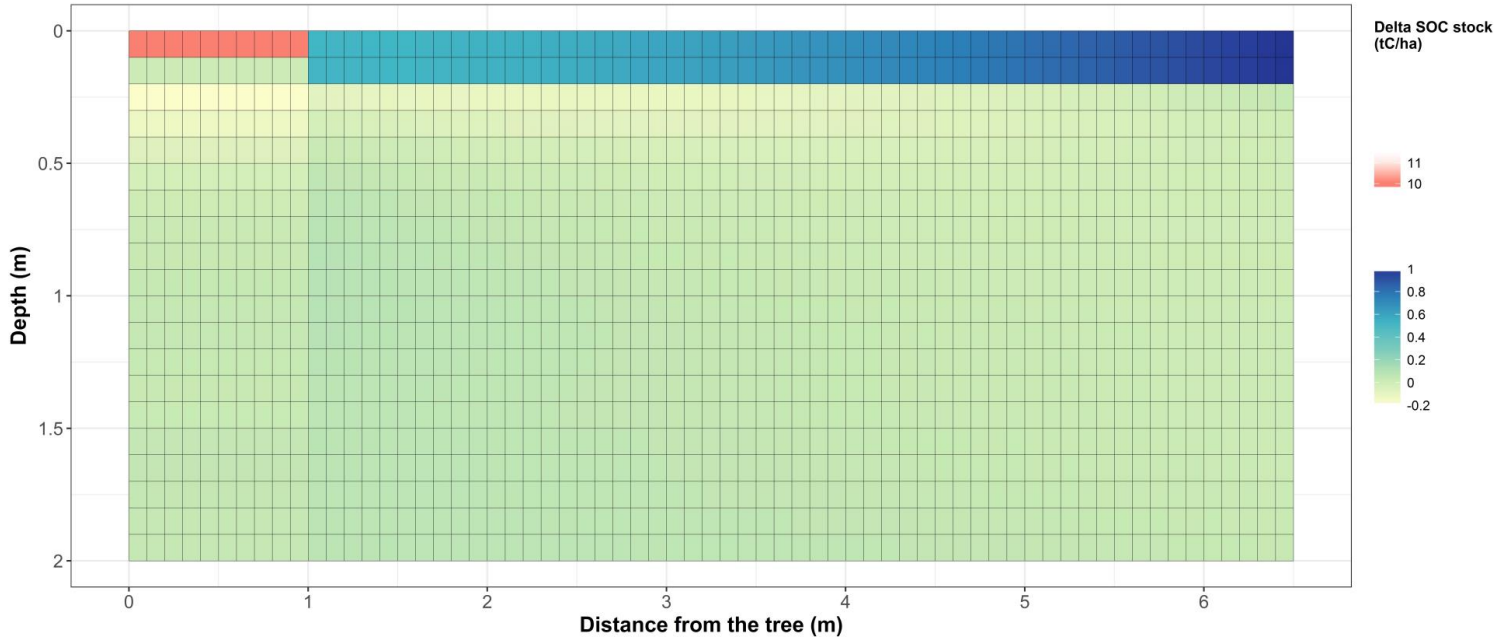

721

722 **Fig. 5.** Spatial distribution of additional SOC storage (t C ha^{-1}) in an 18-year-old silvoarable system compared to an agricultural control plot and

723 represented by the two pools model with priming effect.

Biogeosciences Discuss., doi:10.5194/bg-2017-125, 2017
Manuscript under review for journal Biogeosciences
Discussion started: 12 April 2017

724 **3.4.3 Antagonist effect of priming on SOC storage**

725 The priming effect increases the decomposition rate when more FOC is available. Therefore,
726 the effect of a C inputs increase on SOC storage in the agroforestry plot might be
727 counterbalanced by priming. With our model we were able to estimate the contribution of each
728 driver on SOC storage. The introduction of priming effect in the model reduced the potential
729 SOC storage due to higher organic inputs in the agroforestry system by 91% in the alley, and
730 by 76% in the tree rows (Fig. 6). The potential effect of OC inputs alone on SOC storage was
731 49.12 to 62.77 t C ha^{-1}, but the effect of priming on SOC storage was -44.89 to -47.67 t C ha^{-1},
732 resulting in a modeled SOC storage of 4.23 t C ha^{-1} in the alley and of 15.09 t C ha^{-1} in the tree
733 row down 2 depth (Fig. 6). The negative effect of priming effect on SOC storage increased with
734 increasing soil depth (Fig. S3).

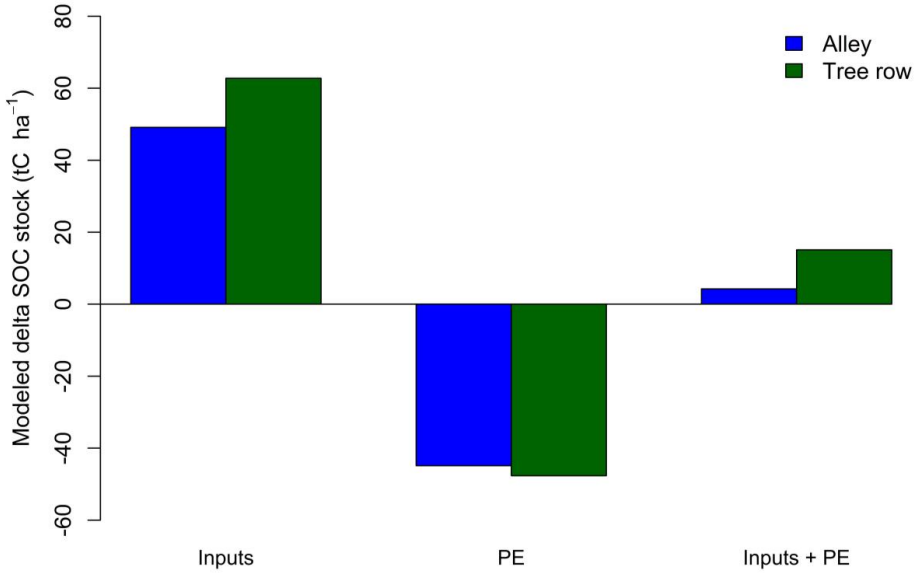

735

736 **Fig. 6.** Decoupling the role of C inputs and priming effect (*PE*) on SOC storage in an 18-year-
737 old silvoarable system down 2 m depth. Inputs: only the input effect is modeled; *PE*:
738 only the priming effect is modeled; Inputs + *PE*: model prediction with both processes
739 taken into account.

Biogeosciences Discuss., doi:10.5194/bg-2017-125, 2017
Manuscript under review for journal Biogeosciences
Discussion started: 12 April 2017

740

741 **4 Discussion**

742 **4.1 OC inputs drive SOC storage in agroforestry systems**

743 Increased SOC stocks in the agroforestry plot compared to the control may be explained either
744 by increased OC inputs, or decreased OC outputs by SOC mineralization, or both. Measured
745 organic carbon inputs to soil were increased by 40% down to 2m depth in the 18-year-old
746 agroforestry plot compared to the control plot. Increased OC inputs in agroforestry systems has
747 been shown in other studies but they were only quantified in the first 20 cm of soil (Oelbermann
748 et al., 2006; Peichl et al., 2006). This study is therefore the first one also quantifying deep OC
749 inputs to soil. In this study and due to a lack of data, soil temperature and soil moisture were
750 considered the same in both plots so that abiotic factors controlling SOC decomposition were
751 identical. The model was able to well reproduce SOC stocks in the agroforestry plot, suggesting
752 that OC inputs is the main driver of SOC storage, and that a decrease of SOC mineralisation
753 due to the agroforestry microclimate is not obvious. Reduced soil temperature is often observed
754 in agroforestry systems (Clinch et al., 2009; Dubbert et al., 2014), but effect of agroforestry on
755 soil moisture is much more complex. The soil evaporation is reduced under the trees, but water
756 is lost through their transpiration (Ilstedt et al., 2016; Ong and Leakey, 1999), and these effects
757 vary with the distance from the tree (Odhiambo et al., 2001). Moreover, the water infiltration
758 and the water storage can be increased under the trees after a rainy event (Anderson et al.,
759 2009). Therefore, the effect of agroforestry on soil moisture is variable in time and space, and
760 should be investigated more in details. Interactions between soil temperature and soil moisture
761 on the SOC decomposition are known to be complex (Conant et al., 2011; Moyano et al., 2013;
762 Sierra et al., 2015) and up to now it is not possible to predict the effect of agroforestry
763 microclimate on the SOC decomposition rate. A sensitivity analysis performed on these two
764 boundary conditions showed that the model was not very sensitive to soil temperature and soil

765 moisture (Fig. S4) suggesting that the potential changes in soil microclimate in the agroforestry
766 plot are not major drivers of the SOC storage. Furthermore, the SOC decomposition rate could
767 also be modified due to an absence of soil tillage in the tree rows (Balesdent et al., 1990) or to
768 an increased aggregate stability (Udawatta et al., 2008) in the topsoil.
769
770 **4.2 Representation of SOC spatial heterogeneity in agroforestry systems**
771 The lateral spatial heterogeneity of SOC stocks in the agroforestry plot was well described by
772 the model, with higher SOC stocks in the tree rows' topsoil than in the alleys. Inputs from the
773 herbaceous vegetation had an important impact on SOC storage in this agroforestry system.
774 The model treated the carbon from this litter as an input to the upper layer of the mineral soil,
775 in the same way as inputs by roots. Introduction of nitrogen in the model could be further tested
776 in order to take into account a lower carbon use efficiency due to a lack of nutrients for
777 microbial growth in this litter. For all models, SOC stocks were better described in the tree rows
778 than in the alleys. In the alleys, the spatial distribution of organic inputs is more complex and
779 thus more difficult to model. The tree root system is influenced by the soil tillage and by the
780 competition with the crop roots, and thus the highest tree fine root density is not observed in
781 the topsoil but in the 0.3-0.5 m soil layer (Cardinael et al., 2015a). In the model, we were not
782 able to represent this specific tree root pattern with commonly used mathematical functions,
783 and tree root profiles were modeled, by default, using a decreasing exponential. Indeed,
784 piecewise linear functions introduce threshold effects not desirable for transport mechanisms,
785 especially diffusion. This simplification could partly explain the model overestimation of SOC
786 stocks in the 0.0-0.1 m layer of the alleys compared to observed data. This result suggests that
787 it could be useful to couple the CARBOSAF model with a model describing root architecture
788 and root growth (Dunbabin et al., 2013; Dupuy et al., 2010), using for instance voxel automata
789 (Mulia et al., 2010). Moreover, the model described a slight increase of SOC stocks in the

middle of the alleys than close to the trees in the alleys. This could be explained by the linear equation used to describe the crop yield as a function of the distance from the trees, leading to an overestimation of the crop yield reduction close to the trees. It could also be explained by the formalism used to model leaf litter distribution in the plot. We considered a homogeneous distribution of leaf inputs in the agroforestry plot, which was the case in the last years, but probably not in the first years of the tree growth where leaves might be more concentrated close to the trees (Thevathasan and Gordon, 1997).

The model also represented a slight SOC storage in the agroforestry plot below 1.0 m depth, but it was not observed in the field. This could be linked to an overestimation of C input from tree fine root mortality. Indeed, a constant root turnover was considered along the soil profile, but several authors reported a decrease of the root turnover with increasing soil depth (Germon et al., 2016; Hendrick and Pregitzer, 1996; Joslin et al., 2006). However, the sensitivity analysis showed that the model was not sensitive to this parameter (Fig. S4).

4.3 Vertical representation of SOC profiles in models

The best model to represent SOC profiles considered the priming effect. This process can act in two different ways on the shape of SOC profiles. It has a direct effect on the SOC mineralization and it therefore modulates the amount of SOC in each soil layer, creating different SOC gradients. This indirectly affects the mechanisms of C transport within the soil profile, as shown by a modification of transport coefficients in the case of priming effect (Table 7). Contrary to what was shown by Cardinael *et al.*, (2015c) in long term bare fallows receiving contrasted organic amendments, the addition of another SOC pool could not surpass the inclusion of priming effect in terms of model performance. Together with Wutzler & Reichstein, (2013) and Guenet *et al.*, (2016), this study therefore suggests that implementing

814 priming effect into SOC models would improve model performances especially when
815 modelling deep SOC profiles.
816 We considered here the same transport coefficients for the FOC and HSOC pools, but the
817 quality and the size of OC particles are different, potentially leading to various movements in
818 the soil by water fluxes or fauna activity (Lavelle, 1997). Moreover, we considered identical
819 transport parameters in the agroforestry and in the control plot, but the presence of trees could
820 modify soil structure, soil water fluxes (Anderson et al., 2009), and the fauna activity (Price
821 and Gordon, 1999). However, the model was little sensitive to these parameters (Fig. S4).
822 Further study could investigate the role of different transport coefficients on the description of
823 SOC profiles.
824
825 **4.4 Higher OC inputs or a different quality of OC?**
826 The introduction of trees in an agricultural field not only modifies the amount of litter residues,
827 but also their quality. Tree leaves, tree roots, and the herbaceous vegetation from the tree row
828 have different C:N ratios, lignin and cellulose contents than the crop residues. Recent studies
829 showed that plant diversity had a positive impact on SOC storage (Lange et al., 2015; Steinbeiss
830 et al., 2008). One of the hypothesis proposed by the authors is that diverse plant communities
831 result in more active, more abundant and more diverse microbial communities, increasing
832 microbial products that can potentially be stabilized. In our model, litter quality is not related
833 to different SOC pools, but is implicitly taken into account in the FOC decomposition rate,
834 which is weighted by the respective contribution from the different types of OC inputs. To test
835 this, we performed a model run considering that all OC inputs in the agroforestry plot were crop
836 inputs (all FOC decomposition rates equaled wheat decomposition rate), but results were not
837 significantly different from the one presented here. We then consider that changes in litter
838 quality in the agroforestry plot did not significantly influence SOC decomposition rates.

839

840 **4.5 Possible limitation of SOC storage by priming effect**

841 Our modelling results showed that the priming effect could considerably reduce the capacity of
842 soils to store organic carbon. Our study showed that the increase of SOC stocks was not
843 proportional to OC inputs, especially at depth. This result has often been observed in Free Air
844 CO_2 Enrichment (FACE) experiments. In these experiments, productivity is usually increased
845 due to CO_2 fertilization, but several authors also reported an increase in SOC decomposition
846 but not linearly linked to the productivity increase (van Groenigen et al., 2014; Sulman et al.,
847 2014). In this study, the estimation of the priming effect intensity was possible because most
848 OC inputs to the soil were accurately measured. The modelled intensity of priming effect was
849 very strong, offsetting 75 to 90% of potential SOC storage due to OC inputs. In a long-term
850 FACE experiment, Carney *et al.*, (2007) also found that SOC decreased due to priming effect,
851 offsetting 52% of additional carbon accumulated in aboveground and coarse root biomass. The
852 priming effect intensity also relies on nutrient availability (Zhang et al., 2013). In agroforestry
853 systems, tree roots can intercept leached nitrate below the crop rooting zone (Andrianarisoa et
854 al., 2016), reducing nutrient availability. This beneficial ecosystem service could indirectly
855 increase the priming effect intensity in deep soil layers.
856 However, this strong intensity could also partially be linked to the formalism used to simulate
857 priming effect. This formalism assumes that there is no mineralisation of the SOC in the
858 absence of fresh OC inputs (no basal respiration). This is a strong hypothesis, but this situation
859 never occurs since the FOC pool is never empty (data not shown). In the alleys and below the
860 maximum rooting depth of crops, there are no direct inputs of FOC, but OC is transported in
861 these deep layers due to transport mechanisms. However, further studies could study the impact
862 of the priming effect formalism on the estimation of its intensity by using explicit microbial
863 biomass for instance (Blagodatsky et al., 2010; Perveen et al., 2014).

Finally, root exudates were not quantified in this study. Several authors showed that they could induce strong priming effects (Bengtson et al., 2012; Keiluweit et al., 2015), but root exudates are also a source of labile carbon, potentially contributing to stable SOC (Cotrufo et al., 2013). These opposing effects of root exudates on SOC should be further investigated, especially concerning the deep roots in agroforestry systems.

5 Conclusions

We proposed the first model that simulates soil organic carbon dynamics in agroforestry accounting for both the whole soil profile and the lateral spatial heterogeneity in agroforestry plots. This model described reasonably well the measured SOC stocks after 18 years of agroforestry and SOC distributions with depth. It showed that the increased inputs of fresh biomass to soil in the agroforestry system explained the observed additional SOC storage and suggested priming effect as a process controlling SOC stocks in the presence of trees. This study points out at processes that may be modified by deep rooting trees and deserve further studies given their potential effects on SOC dynamics, such as additional inputs of C as roots exudates, or altered soil structure leading to modified SOC transport rates.

6 Data availability

The data and the model are freely available upon request and can be obtained by contacting the author (remi.cardinael@cirad.fr).

Information about the Supplement

The Supplement includes the different model performances (Table S1), the potential SOC decomposition rate as a function of soil depth (Fig. S1), the correlation matrix of optimized

parameters (Fig. 8), the decoupling of OC inputs and priming effect as a function of soil depth (Fig. S3), and a sensitivity analysis of the model (Fig. S4).

Acknowledgments.

This study was financed by the French Environment and Energy Management Agency (ADEME), following a call for proposals as part of the REACCTIF program (Research on Climate Change Mitigation in Agriculture and Forestry). This work was part of the funded project AGRIPSOL (Agroforestry for Soil Protection, 1260C0042), coordinated by Agroof. Rémi Cardinael was supported both by ADEME and by La Fondation de France. We thank the farmer, Mr Breton, who allowed us to sample in his field. We are very grateful to our colleagues for their work in the field since the tree planting, especially Jean-François Bourdoncle, Myriam Dauzat, Lydie Dufour, Jonathan Mineau, Alain Sellier and Benoit Suard. We thank colleagues and students who helped us for measurements in the field or in the laboratory, especially Daniel Billiou, Cyril Girardin, Patricia Mahafaka, Agnès Martin, Valérie Pouteau, Alexandre Rosa, and Manon Villeneuve. Finally, we would like to thank Jérôme Balesdent and Pierre Barré for their valuable comments on the modeling part of this work.

References

Ahrens, B., Braakhekke, M. C., Guggenberger, G., Schrumpf, M. and Reichstein, M.: Contribution of sorption, DOC transport and microbial interactions to the ^{14}C age of a soil organic carbon profile: Insights from a calibrated process model, Soil Biol. Biochem., 88, 390–402, 2015.

Albrecht, A. and Kandji, S. T.: Carbon sequestration in tropical agroforestry systems, Agric. Ecosyst. Environ., 99, 15–27, 2003.

Anderson, S. H., Udawatta, R. P., Seobi, T. and Garrett, H. E.: Soil water content and infiltration

913 in agroforestry buffer strips, Agrofor. Syst., 75(1), 5–16, 2009.

914 Andrianarisoa, K., Dufour, L., Bienaime, S., Zeller, B. and Dupraz, C.: The introduction of
915 hybrid walnut trees (*Juglans nigra* x *regia* cv. NG23) into cropland reduces soil mineral N
916 content in autumn in southern France, Agrofor. Syst., 90(2), 193–205, 2016.

917 Baisden, W. T. and Parfitt, R. L.: Bomb ^{14}C enrichment indicates decadal C pool in deep soil?,
918 Biogeochemistry, 85, 59–68, , 2007.

919 Baisden, W. T., Amundson, R., Brenner, D. L., Cook, A. C., Kendall, C. and Harden, J. W.: A
920 multiisotope C and N modeling analysis of soil organic matter turnover and transport as a
921 function of soil depth in a California annual grassland soil chronosequence, Global
922 Biogeochem. Cycles, 16(4), 82-1-82–26, 2002.

923 Balandier, P. and Dupraz, C.: Growth of widely spaced trees. A case study from young
924 agroforestry plantations in France, Agrofor. Syst., 43, 151–167, 1999.

925 Balesdent, J., Mariotti, A. and Boisgontier, D.: Effect of tillage on soil organic carbon
926 mineralization estimated from ^{13}C abundance in maize fields, J. Soil Sci., 41(4), 587–596, 1990.

927 Bambrick, A. D., Whalen, J. K., Bradley, R. L., Cogliastro, A., Gordon, A. M., Olivier, A. and
928 Thevathasan, N. V: Spatial heterogeneity of soil organic carbon in tree-based intercropping
929 systems in Quebec and Ontario, Canada, Agrofor. Syst., 79, 343–353, 2010.

930 Bengtson, P., Barker, J. and Grayston, S. J.: Evidence of a strong coupling between root
931 exudation, C and N availability, and stimulated SOM decomposition caused by rhizosphere
932 priming effects, Ecol. Evol., 2(8), 1843–1852, 2012.

933 Blagodatsky, S., Blagodatskaya, E., Yuyukina, T. and Kuzyakov, Y.: Model of apparent and
934 real priming effects: Linking microbial activity with soil organic matter decomposition, Soil
935 Biol. Biochem., 42(8), 1275–1283, 2010.

936 Braakhekke, M. C., Beer, C., Hoosbeek, M. R., Reichstein, M., Kruijt, B., Schrumpf, M. and

937 Kabat, P.: SOMPROF: A vertically explicit soil organic matter model, Ecol. Modell., 222(10),
938 1712–1730, 2011.

939 Bruun, S., Christensen, B. T., Thomsen, I. K., Jensen, E. S. and Jensen, L. S.: Modeling vertical
940 movement of organic matter in a soil incubated for 41 years with ^{14}C labeled straw, Soil Biol.
941 Biochem., 39(1), 368–371, 2007.

942 Burgess, P. J., Incoll, L. D., Corry, D. T., Beaton, A. and Hart, B. J.: Poplar (*Populus* spp)
943 growth and crop yields in a silvoarable experiment at three lowland sites in England, Agrofor.
944 Syst., 63, 157–169, 2004.

945 Cardinael, R., Mao, Z., Prieto, I., Stokes, A., Dupraz, C., Kim, J. H. and Jourdan, C.:
946 Competition with winter crops induces deeper rooting of walnut trees in a Mediterranean alley
947 cropping agroforestry system, Plant Soil, 391, 219–235, 2015a.

948 Cardinael, R., Chevallier, T., Barthès, B. G., Saby, N. P. A., Parent, T., Dupraz, C., Bernoux,
949 M. and Chenu, C.: Impact of alley cropping agroforestry on stocks, forms and spatial
950 distribution of soil organic carbon - A case study in a Mediterranean context, Geoderma, 259–
951 260, 288–299, 2015b.

952 Cardinael, R., Eglin, T., Guenet, B., Neill, C., Houot, S. and Chenu, C.: Is priming effect a
953 significant process for long-term SOC dynamics? Analysis of a 52-years old experiment,
954 Biogeochemistry, 123, 203–219, 2015c.

955 Cardinael, R., Chevallier, T., Cambou, A., Béral, C., Barthès, B. G., Dupraz, C., Durand, C.,
956 Kouakoua, E. and Chenu, C.: Increased soil organic carbon stocks under agroforestry: A survey
957 of six different sites in France, Agric. Ecosyst. Environ., 236, 243–255, 2017.

958 Carney, K. M., Hungate, B. A., Drake, B. G. and Megonigal, J. P.: Altered soil microbial
959 community at elevated CO2 leads to loss of soil carbon, PNAS, 104(12), 4990–4995, 2007.

960 Charbonnier, F., le Maire, G., Dreyer, E., Casanoves, F., Christina, M., Dauzat, J., Eitel, J. U.

961 H., Vaast, P., Vierling, L. A. and Roupsard, O.: Competition for light in heterogeneous
962 canopies: Application of MAESTRA to a coffee (*Coffea arabica* L.) agroforestry system,
963 Agric. For. Meteorol., 181, 152–169, 2013.

964 Chaudhry, A. K., Khan, G. S., Siddiqui, M. T., Akhtar, M. and Aslam, Z.: Effect of arable crops
965 on the growth of poplar (*Populus deltoides*) tree in agroforestry system, Pakistan J. Agric. Sci.,
966 40, 82–85, 2003.

967 Chifflot, V., Bertoni, G., Cabanettes, A. and Gavaland, A.: Beneficial effects of intercropping
968 on the growth and nitrogen status of young wild cherry and hybrid walnut trees, Agrofor. Syst.,
969 66(1), 13–21, 2006.

970 Clinch, R. L., Thevathasan, N. V., Gordon, A. M., Volk, T. A. and Sidders, D.: Biophysical
971 interactions in a short rotation willow intercropping system in southern Ontario, Canada, Agric.
972 Ecosyst. Environ., 131(1–2), 61–69, 2009.

973 Conant, R. T., Ryan, M. G., Ågren, G. I., Birge, H. E., Davidson, E. A., Eliasson, P. E., Evans,
974 S. E., Frey, S. D., Giardina, C. P., Hopkins, F. M., Hyvönen, R., Kirschbaum, M. U. F.,
975 Lavallee, J. M., Leifeld, J., Parton, W. J., Megan Steinweg, J., Wallenstein, M. D., Martin
976 Wetterstedt, J. Å. and Bradford, M. A.: Temperature and soil organic matter decomposition
977 rates - synthesis of current knowledge and a way forward, Glob. Chang. Biol., 17(11), 3392–
978 3404, 2011.

979 Cotrufo, M. F., Wallenstein, M. D., Boot, C. M., Denef, K. and Paul, E.: The Microbial
980 Efficiency-Matrix Stabilization (MEMS) framework integrates plant litter decomposition with
981 soil organic matter stabilization: do labile plant inputs form stable soil organic matter?, Glob.
982 Chang. Biol., 19(4), 988–95, 2013.

983 Davidson, E. A. and Janssens, I. A.: Temperature sensitivity of soil carbon decomposition and
984 feedbacks to climate change, Nature, 440, 165–173, 2006.

985 Dimassi, B., Cohan, J.-P., Labreuche, J. and Mary, B.: Changes in soil carbon and nitrogen
986 following tillage conversion in a long-term experiment in Northern France, Agric. Ecosyst.
987 Environ., 169, 12–20, 2013.

988 Dubbert, M., Mosena, A., Piayda, A., Cuntz, M., Correia, A. C., Pereira, J. S. and Werner, C.:
989 Influence of tree cover on herbaceous layer development and carbon and water fluxes in a
990 Portuguese cork-oak woodland, Acta Oecologica, 59, 35–45, 2014.

991 Dufour, L., Metay, A., Talbot, G. and Dupraz, C.: Assessing Light Competition for Cereal
992 Production in Temperate Agroforestry Systems using Experimentation and Crop Modelling, J.
993 Agron. Crop Sci., 199(3), 217–227, 2013.

994 Dunbabin, V. M., Postma, J. A., Schnepf, A., Pagès, L., Javaux, M., Wu, L., Leitner, D., Chen,
995 Y. L., Rengel, Z. and Diggle, A. J.: Modelling root-soil interactions using three-dimensional
996 models of root growth, architecture and function, Plant Soil, 372(1–2), 93–124, 2013.

997 Dupuy, L., Gregory, P. J. and Bengough, A. G.: Root growth models: Towards a new generation
998 of continuous approaches, J. Exp. Bot., 61(8), 2131–2143, 2010.

999 Duursma, R.A. and Medlyn, B.E.: MAESPA: a model to study interactions between water
1000 limitation, environmental drivers and vegetation function at tree and stand levels, with an
1001 example application to [CO_2] × drought interactions, Geosci. Model Dev., 5, 919–940, 2012.

1002 Eilers, K. G., Debenport, S., Anderson, S. and Fierer, N.: Digging deeper to find unique
1003 microbial communities: The strong effect of depth on the structure of bacterial and archaeal
1004 communities in soil, Soil Biol. Biochem., 50, 58–65, 2012.

1005 Eissenstat, D. M. and Yanai, R. D.: The Ecology of Root Lifespan, Adv. Ecol. Res., 27, 1–60,
1006 1997.

1007 Ellert, B. H. and Bettany, J. R.: Calculation of organic matter and nutrients stored in soils under
1008 contrasting management regimes, Can. J. Soil Sci., 75, 529–538, 1995.

1009 Elzein, A. and Balesdent, J.: Mechanistic simulation of vertical distribution of carbon
1010 concentrations and residence times in soils, Soil Sci. Soc. Am. J., 59, 1328–1335, 1995.

1011 Fierer, N., Schimel, J. P. and Holden, P. A.: Variations in microbial community composition
1012 through two soil depth profiles, Soil Biol. Biochem., 35(1), 167–176, 2003.

1013 Fontaine, S., Barot, S., Barré, P., Bdioui, N., Mary, B. and Rumpel, C.: Stability of organic
1014 carbon in deep soil layers controlled by fresh carbon supply, Nature, 450, 277–281, 2007.

1015 Germon, A., Cardinael, R., Prieto, I., Mao, Z., Kim, J. H., Stokes, A., Dupraz, C., Laclau, J.-P.
1016 and Jourdan, C.: Unexpected phenology and lifespan of shallow and deep fine roots of walnut
1017 trees grown in a silvoarable Mediterranean agroforestry system, Plant Soil, 401, 409–426, 2016.

1018 Graves, A. R., Burgess, P. J., Palma, J. H. N., Herzog, F., Moreno, G., Bertomeu, M., Dupraz,
1019 C., Liagre, F., Keesman, K., van der Werf, W., de Nooy, A. K. and van den Briel, J. P.:
1020 Development and application of bio-economic modelling to compare silvoarable, arable, and
1021 forestry systems in three European countries, Ecol. Eng., 29(4), 434–449, 2007.

1022 Graves, A. R., Burgess, P. J., Palma, J., Keesman, K. J., van der Werf, W., Dupraz, C., van
1023 Keulen, H., Herzog, F. and Mayus, M.: Implementation and calibration of the parameter-sparse
1024 Yield-SAFE model to predict production and land equivalent ratio in mixed tree and crop
1025 systems under two contrasting production situations in Europe, Ecol. Modell., 221, 1744–1756,
1026 2010.

1027 van Groenigen, K. J., Qi, X., Osenberg, C. W., Luo, Y. and Hungate, B. A.: Faster
1028 decomposition under increased atmospheric CO_2 limits soil carbon storage, Science,
1029 344(6183), 508–9, 2014.

1030 Guenet, B., Eglin, T., Vasilyeva, N., Peylin, P., Ciais, P. and Chenu, C.: The relative importance
1031 of decomposition and transport mechanisms in accounting for soil organic carbon profiles,
1032 Biogeosciences, 10(4), 2379–2392, 2013.

1033 Guenet, B., Moyano, F. E., Peylin, P., Ciais, P. and Janssens, I. A.: Towards a representation
1034 of priming on soil carbon decomposition in the global land biosphere model ORCHIDEE
1035 (version 1.9.5.2), Geosci. Model Dev., 9, 841–855, 2016.

1036 Haile, S. G., Nair, V. D. and Nair, P. K. R.: Contribution of trees to carbon storage in soils of
1037 silvopastoral systems in Florida, USA, Glob. Chang. Biol., 16, 427–438, 2010.

1038 Hendrick, R. L. and Pregitzer, K. S.: Temporal and depth-related patterns of fine root dynamics
1039 in northern hardwood forests, J. Ecol., 84, 167–176, 1996.

1040 Howlett, D. S., Moreno, G., Mosquera Losada, M. R., Nair, P. K. R. and Nair, V. D.: Soil
1041 carbon storage as influenced by tree cover in the Dehesa cork oak silvopasture of central-
1042 western Spain, J. Environ. Monit., 13(7), 1897–904, 2011.

1043 Ilstedt, U., Bargués Tobella, A., Bazié, H. R., Bayala, J., Verbeeten, E., Nyberg, G., Sanou, J.,
1044 Benegas, L., Murdiyarso, D., Laudon, H., Sheil, D. and Malmer, A.: Intermediate tree cover
1045 can maximize groundwater recharge in the seasonally dry tropics, Sci. Rep., 6, 21930, 2016.

1046 IUSS Working Group WRB: World Reference Base for Soil Resources 2006, first update 2007.
1047 World Soil Resources Reports No. 103. FAO, Rome., 2007.

1048 Jobbagy, E. G. and Jackson, R. B.: The vertical distribution of soil organic carbon and its
1049 relation to climate and vegetation, Ecol. Appl., 10, 423–436, 2000.

1050 Joslin, J. D., Gaudinski, J. B., Torn, M. S., Riley, W. J. and Hanson, P. J.: Fine-root turnover
1051 patterns and their relationship to root diameter and soil depth in a ^{14}C-labeled hardwood forest,
1052 New Phytol., 172, 523–535, 2006.

1053 Kätterer, T., Bolinder, M. A., Andrén, O., Kirchmann, H. and Menichetti, L.: Roots contribute
1054 more to refractory soil organic matter than above-ground crop residues, as revealed by a long-
1055 term field experiment, Agric. Ecosyst. Environ., 141, 184–192, 2011.

1056 Keiluweit, M., Bougoure, J. J., Nico, P. S., Pett-Ridge, J., Weber, P. K. and Kleber, M.: Mineral

protection of soil carbon counteracted by root exudates, Nat. Clim. Chang., 5, 588-595, 2015.

Kim, D.-G., Kirschbaum, M. U. F. and Beedy, T. L.: Carbon sequestration and net emissions of CH4 and N2O under agroforestry: Synthesizing available data and suggestions for future studies, Agric. Ecosyst. Environ., 226, 65–78, 2016.

Koarashi, J., Hockaday, W. C., Masiello, C. A. and Trumbore, S. E.: Dynamics of decadally cycling carbon in subsurface soils, J. Geophys. Res., 117, 1–13, 2012.

Koven, C. D., Riley, W. J., Subin, Z. M., Tang, J. Y., Torn, M. S., Collins, W. D., Bonan, G. B., Lawrence, D. M. and Swenson, S. C.: The effect of vertically resolved soil biogeochemistry and alternate soil C and N models on C dynamics of CLM4, Biogeosciences, 10(11), 7109–7131, 2013.

Lange, M., Eisenhauer, N., Sierra, C. A., Bessler, H., Engels, C., Griffiths, R. I., Mellado-Vázquez, P. G., Malik, A. A., Roy, J., Scheu, S., Steinbeiss, S., Thomson, B. C., Trumbore, S. E. and Gleixner, G.: Plant diversity increases soil microbial activity and soil carbon storage, Nat. Commun., 6, 6707, 2015.

Lavelle, P.: Faunal activities and soil processes: adaptative strategy that determine ecosystem function., 1997.

Li, F., Meng, P., Fu, D. and Wang, B.: Light distribution, photosynthetic rate and yield in a Paulownia-wheat intercropping system in China, Agrofor. Syst., 74(2), 163–172, 2008.

Lorenz, K. and Lal, R.: Soil organic carbon sequestration in agroforestry systems. A review, Agron. Sustain. Dev., 34, 443–454, 2014.

Luedeling, E., Smethurst, P. J., Baudron, F., Bayala, J., Huth, N. I., van Noordwijk, M., Ong, C. K., Mulia, R., Lusiana, B., Muthuri, C. and Sinclair, F. L.: Field-scale modeling of tree-crop interactions: Challenges and development needs, Agric. Syst., 142, 51–69, 2016.

Mead, R. and Willey, R. W.: The concept of a “land equivalent ratio” and advantages in yields

from intercropping, Exp. Agric., 16(3), 217–228, 1980.

Moreno, G., Obrador, J. J., Cubera, E. and Dupraz, C.: Fine root distribution in Dehesas of central-western Spain, Plant Soil, 277(1–2), 153–162, 2005.

Moyano, F. E., Vasilyeva, N., Bouckaert, L., Cook, F., Craine, J., Curiel Yuste, J., Don, A., Epron, D., Formanek, P., Franzluebbers, A., Ilstedt, U., Kätterer, T., Orchard, V., Reichstein, M., Rey, A., Ruamps, L., Subke, J. A., Thomsen, I. K. and Chenu, C.: The moisture response of soil heterotrophic respiration: Interaction with soil properties, Biogeosciences, 9, 1173–1182, 2012.

Moyano, F. E., Manzoni, S. and Chenu, C.: Responses of soil heterotrophic respiration to moisture availability: An exploration of processes and models, Soil Biol. Biochem., 59, 72–85, 2013.

Mulia, R. and Dupraz, C.: Unusual fine root distributions of two deciduous tree species in southern France: What consequences for modelling of tree root dynamics?, Plant Soil, 281, 71–85, 2006.

Mulia, R., Dupraz, C. and van Noordwijk, M.: Reconciling root plasticity and architectural ground rules in tree root growth models with voxel automata, Plant Soil, 337(1–2), 77–92, 2010.

Nair, P. K.: An introduction to agroforestry, Kluwer, Dordrecht, The Netherlands., 1993.

Nair, P. K. R.: Classification of agroforestry systems, Agrofor. Syst., 3(2), 97–128, 1985.

van Noordwijk, M. and Lusiana, B.: WaNuLCAS, a model of water, nutrient and light capture in agroforestry systems, Agrofor. Syst., 43, 217–242, 1999.

Odhiambo, H. O., Ong, C. K., Deans, J. D., Wilson, J., Khan, A. A. H. and Sprent, J. I.: Roots, soil water and crop yield: Tree crop interactions in a semi-arid agroforestry system in Kenya, Plant Soil, 235(2), 221–233, 2001.

Oelbermann, M. and Voroney, R. P.: And evaluation of the century model to predict soil

1105 organic carbon: examples from Costa Rica and Canada, Agrofor. Syst., 82, 37–50, 2011.

1106 Oelbermann, M., Voroney, R. P. and Gordon, A. M.: Carbon sequestration in tropical and
1107 temperate agroforestry systems: a review with examples from Costa Rica and southern Canada,
1108 Agric. Ecosyst. Environ., 104, 359–377, 2004.

1109 Oelbermann, M., Voroney, R. P., Thevathasan, N. V., Gordon, A. M., Kass, D. C. L. and
1110 Schlönvoigt, A. M.: Soil carbon dynamics and residue stabilization in a Costa Rican and
1111 southern Canadian alley cropping system, Agrofor. Syst., 68(1), 27–36, 2006.

1112 Ong, C. K. and Leakey, R. R. B.: Why tree-crop interactions in agroforestry appear at odds with
1113 tree-grass interactions in tropical savannahs, Agrofor. Syst., 45(1–3), 109–129, 1999.

1114 Parton, W. J., Schimel, D. S., Cole, C. V and Ojima, D. S.: Analysis of factors controlling soil
1115 organic matter levels in great plains grasslands, Soil Sci. Soc. Am. J., 51, 1173–1179, 1987.

1116 Peichl, M., Thevathasan, N. V, Gordon, A. M., Huss, J. and Abohassan, R. A.: Carbon
1117 sequestration potentials in temperate tree-based intercropping systems, southern Ontario,
1118 Canada, Agrofor. Syst., 66, 243–257, 2006.

1119 Perveen, N., Barot, S., Alvarez, G., Klumpp, K., Martin, R., Rapaport, A., Herfurth, D.,
1120 Louault, F. and Fontaine, S.: Priming effect and microbial diversity in ecosystem functioning
1121 and response to global change: A modeling approach using the SYMPHONY model, Glob.
1122 Chang. Biol., 20(4), 1174–1190, 2014.

1123 Price, G. W. and Gordon, A. M.: Spatial and temporal distribution of earthworms in a temperate
1124 intercropping system in southern Ontario, Canada, Agrofor. Syst., 44, 141–149, 1999.

1125 Prieto, I., Roumet, C., Cardinael, R., Kim, J., Maeght, J.-L., Mao, Z., Portillo, N.,
1126 Thammahacksa, C., Dupraz, C., Jourdan, C., Pierret, A., Roupsard, O. and Stokes, A.: Root
1127 functional parameters along a land-use gradient: evidence of a community-level economics
1128 spectrum, J. Ecol., 103, 361–373, 2015.

1129 Prieto, I., Stokes, A. and Roumet, C.: Root functional parameters predict fine root
1130 decomposability at the community level, J. Ecol., 104, 725–733, 2016.

1131 R Development Core Team: R: A language and environment for statistical computing, 2013.

1132 Rasse, D. P., Mulder, J., Moni, C. and Chenu, C.: Carbon turnover kinetics with depth in a
1133 French loamy soil, Soil Sci. Soc. Am. J., 70, 2097–2105, 2006.

1134 Salomé, C., Nunan, N., Pouteau, V., Lerch, T. Z. and Chenu, C.: Carbon dynamics in topsoil
1135 and in subsoil may be controlled by different regulatory mechanisms, Glob. Chang. Biol., 16,
1136 416–426, 2010.

1137 Santaren, D., Peylin, P., Viovy, N. and Ciais, P.: Optimizing a process-based ecosystem model
1138 with eddy-covariance flux measurements: A pine forest in southern France, Global
1139 Biogeochem. Cycles, 21, 1–15, 2007.

1140 Shahzad, T., Chenu, C., Genet, P., Barot, S., Perveen, N., Mougin, C. and Fontaine, S.:
1141 Contribution of exudates, arbuscular mycorrhizal fungi and litter depositions to the rhizosphere
1142 priming effect induced by grassland species, Soil Biol. Biochem., 80, 146–155, 2015.

1143 Sierra, C. A., Trumbore, S. E., Davidson, E. A., Vicca, S. and Janssens, I.: Sensitivity of
1144 decomposition rates of soil organic matter with respect to simultaneous changes in temperature
1145 and moisture, J. Adv. Model. Earth Syst., 7, 335–356, 2015.

1146 Somarriba, E.: Revisiting the past: an essay on agroforestry definition, Agrofor. Syst., 19(3),
1147 233–240, 1992.

1148 Steinbeiss, S., Beßler, H., Engels, C., Temperton, V. M., Buchmann, N., Roscher, C.,
1149 Kreutziger, Y., Baade, J., Habekost, M. and Gleixner, G.: Plant diversity positively affects
1150 short-term soil carbon storage in experimental grasslands, Glob. Chang. Biol., 14(12), 2937–
1151 2949, 2008.

1152 Sulman, B. N., Phillips, R. P., Oishi, A. C., Shevliakova, E. and Pacala, S. W.: Microbe-driven

1153 turnover offsets mineral-mediated storage of soil carbon under elevated CO2, Nat. Clim.
1154 Chang., 4, 1099–1102, 2014.

1155 Taghizadeh-Toosi, A., Christensen, B. T., Hutchings, N. J., Vejlin, J., Kätterer, T., Glendining,
1156 M. and Olesen, J. E.: C-TOOL: A simple model for simulating whole-profile carbon storage in
1157 temperate agricultural soils, Ecol. Modell., 292, 11–25, 2014.

1158 Talbot, G.: L'intégration spatiale et temporelle du partage des ressources dans un système
1159 agroforestier noyers-céréales: une clef pour en comprendre la productivité ?, PhD Dissertation,
1160 Université Montpellier II., 2011.

1161 Tarantola, A.: Inverse problem theory: methods for data fitting and model parameter estimation,
1162 edited by Elsevier., 1987.

1163 Tarantola, A.: Inverse Problem Theory and Methods for Model Parameter Estimation, edited
1164 by SIAM., 2005.

1165 Thevathasan, N. V. and Gordon, A. M.: Poplar leaf biomass distribution and nitrogen dynamics
1166 in a poplar-barley intercropped system in southern Ontario, Canada, Agrofor. Syst., 37(1995),
1167 79–90, 1997.

1168 Udawatta, R. P., Kremer, R. J., Adamson, B. W. and Anderson, S. H.: Variations in soil
1169 aggregate stability and enzyme activities in a temperate agroforestry practice, Appl. Soil Ecol.,
1170 39(2), 153–160, 2008.

1171 Virto, I., Barré, P., Burlot, A. and Chenu, C.: Carbon input differences as the main factor
1172 explaining the variability in soil organic C storage in no-tilled compared to inversion tilled
1173 agrosystems, Biogeochemistry, 108, 17–26, 2012.

1174 van der Werf, W., Keesman, K., Burgess, P., Graves, A., Pilbeam, D., Incoll, L. D., Metselaar,
1175 K., Mayus, M., Stappers, R., van Keulen, H., Palma, J. and Dupraz, C.: Yield-SAFE: A
1176 parameter-sparse, process-based dynamic model for predicting resource capture, growth, and

production in agroforestry systems, Ecol. Eng., 29(4), 419–433, 2007.

Wutzler, T. and Reichstein, M.: Colimitation of decomposition by substrate and decomposers - a comparison of model formulations, Biogeosciences, 5, 749–759, 2008.

Wutzler, T. and Reichstein, M.: Priming and substrate quality interactions in soil organic matter models, Biogeosciences, 10(3), 2089–2103, 2013.

Yin, R. and He, Q.: The spatial and temporal effects of paulownia intercropping: The case of northern China, Agrofor. Syst., 37, 91–109, 1997.

Zhang, W., Wang, X. and Wang, S.: Addition of external organic carbon and native soil organic carbon decomposition: a meta-analysis., PLoS One, 8(2), e54779, 2013.